Journal of Visualized Experiments

In situ Grazing Incidence Small Angle X-ray Scattering on Roll-To-Roll Coating of Organic Solar Cells with Laboratory X-ray Instrumentation.

--Manuscript Draft--

Article Type:	Methods Article - JoVE Produced Video
Manuscript Number:	JoVE61374R2
Full Title:	In situ Grazing Incidence Small Angle X-ray Scattering on Roll-To-Roll Coating of Organic Solar Cells with Laboratory X-ray Instrumentation.
Section/Category:	JoVE Engineering
Keywords:	in situ GISAXS; organic solar cells; non-fullerene acceptor; roll-to-roll coating; Teubner-Strey; drying kinetics
Corresponding Author:	Jens Andreasen DENMARK
Corresponding Author's Institution:	
Corresponding Author E-Mail:	jewa@dtu.dk
Order of Authors:	Michael Korning Sørensen
	Moises Espindola Rodriguez
	Marcial Fernández Castro
	Ashwin Nambi
	Luise Theil Kuhn
	Jens Wenzel Andreasen
Additional Information:	
Question	**Response**
Please indicate whether this article will be Standard Access or Open Access.	Standard Access (US$2,400)
Please indicate the **city, state/province, and country** where this article will be **filmed**. Please do not use abbreviations.	Roskilde, Denmark

TITLE:

In situ Grazing Incidence Small Angle X-ray Scattering on Roll-To-Roll Coating of Organic Solar Cells with Laboratory X-ray Instrumentation

AUTHORS:

Michael Korning Sørensen, Moises Espindola Rodriguez, Marcial Fernández Castro, Ashwin Nambi, Luise Theil Kuhn, Jens Wenzel Andreasen

Department of Energy Conversion and Storage, Technical University of Denmark, Kongens Lyngby, Denmark.

Michael K. Sørensen (mkso@dtu.dk)
Moises E. Rodriguez (mesro@dtu.dk)
Marcial Fernández Castro (marfca@dtu.dk)
Ashwin Nambi (s181252@student.dtu.dk)
Luise T. Kuhn (luku@dtu.dk)

CORRESPONDING AUTHOR

Jens W. Andreasen (jewa@dtu.dk)

KEYWORDS

in situ GISAXS, organic solar cells, non-fullerene acceptor, roll-to-roll coating, Teubner-Strey, drying kinetics

SUMMARY

This paper is a demonstration and a guideline to perform and analyze in-house (with a laboratory X-ray instrument) in situ GISAXS experiments of drying inks on roll-to-roll slot-die coated, non-fullerene organic photovoltaics.

ABSTRACT

We present an in-house, in situ Grazing Incidence Small Angle X-ray Scattering (GISAXS) experiment, developed to probe the drying kinetics of roll-to-roll slot-die coating of the active layer in organic photovoltaics (OPVs), during deposition. For this demonstration, the focus is on the combination of **P3HT:O-IDTBR** and **P3HT:EH-IDTBR**, which have different drying kinetics and device performance, despite their chemical structure only varying slightly by the sidechain of the small molecule acceptor. This article provides a step-by-step guide to perform an in situ GISAXS experiment and demonstrates how to analyze and interpret the results. Usually, performing this type of in situ X-ray experiments to investigate the drying kinetics of the active layer in OPVs relies on access to synchrotrons. However, by using and further developing the method described in this paper, it is possible to perform experiments with a coarse temporal and spatial resolution, on a day-to-day basis to gain fundamental insight in the morphology of drying inks.

INTRODUCTION:

Organic photovoltaics (OPVs) represents one of the most promising emerging solar cell technologies. OPVs can enable large-scale production of a cost-effective renewable energy source based on nontoxic materials with remarkable short energy payback times[1]. The photoactive part in OPVs is an approximately 300-400 nm thick layer of conductive polymers and molecules, which can be printed at a rate of several meters per minute by roll-to-roll coating techniques[1]. This thin-film technology is flexible, colorful, and lightweight, which opens paths for new solar energy markets, such as Internet-of-Things, building integration, decorative installations and fast installation/uninstallation at very large scale[2–5]. Furthermore, OPVs consist solely of abundant and nontoxic elements, which make them both cheap to produce and recycle. Therefore, this technology is receiving increasing attention from industry and academia. Tremendous efforts have been made to optimize each layer in the complete stack that constitutes the organic solar cell, and a lot of theoretical and experimental research has been done to understand the underlying physics of OPVs[6–8]. The enormous interest in the technology has pushed the field to its current state where champion devices fabricated in laboratories are exceeding 18% efficiency[9]. However, upscaling the fabrication (i.e., moving from spin-coating on rigid substrates to scalable deposition on flexible substrates) is accompanied by significant losses in efficiency[10]. Bridging this gap is thus paramount for OPVs to become competitive with other commercially available thin-film solar cell technologies.

OPV is a thin-film technology that consists of several functional layers. In this demonstration, the focus is solely on the photoactive layer. This layer is particularly important, as this is where the photons are absorbed, and the photocurrent is generated. Typically, the photoactive layer consists of at least two constituents, namely a donor and an acceptor. Here, the focus is on the donor polymer **P3HT** in combination with either **O-IDTBR** or **EH:IDTBR** as the acceptor[11], with the chemical formulas as shown in **Figure 1**. The optimal design of the photoactive layer is described as a bulk heterojunction (BHJ), where the compounds are intermixed throughout the device, as shown in **Figure 2**. The BHJ is obtained by slot-die coating an ink consisting of the donor and the acceptor in solution[10]. While coating the wet ink onto the substrate, the solvent molecules evaporate, which leaves the donor and acceptor in an intermixed state. The distribution of donor/acceptor with respect to phase separation, orientation, ordering, and size distribution, is commonly referred to as the morphology of the BHJ. The morphology of the active layer plays a significant role in the solar cell performance due to the nature of the working principle[4,12]. The working principle is illustrated in **Figure 2** and can be described in four steps: First, an incoming photon is absorbed and excites an electron from the highest occupied molecular orbital (HOMO) to the lowest unoccupied molecular orbital (LUMO). The hole (a vacant state in the HOMO) and the excited electron are bound together. This bound electron-hole-pair is referred to as an exciton. Second, the exciton is free to move around, and the approximate mean free path before recombination is 20 nm[6]. Third, when the exciton is near an interface between donor and acceptor, it is energetically favorable to dissociate into a free electron in the LUMO of the acceptor and a free hole in the HOMO of the donor. Fourth, if the device is connected to a circuit, charges will thereby be transported to the anode and cathode. To improve the functionality of OPVs, the morphology must be optimized to accommodate each of the four steps to ensure that the BHJ absorbs as many of the incoming photons as possible and generates as many moving charges as possible. The big scientific question of the optimal morphology remains.

This is still an open question, and the procedure for optimizing the morphology for a specific combination of donor and acceptor is so far done by trial and error. Optimal coating conditions for the blend **P3HT:O-IDTBR** and **P3HT:EH-IDTBR** have been reported[13,14]. Similar experimental parameters were used here to prepare both **P3HT:O-IDTBR** and **P3HT:EH-IDTBR** roll-coated on a flexible substrate at 60 °C, as described by Kuan Liu et al.[15]. The roll-coated OPVs have an inverted structure[16] and were fabricated on flexible substrates without indium tin oxide (ITO-free), with the structure PET/Ag-grid/PEDOT:PSS/ZnO/**P3HT:O-IDTBR** or **EH-IDTBR/**PEDOT:PSS/Ag-grid, where the light enters through the PET substrate. PEDOT:PSS is an abbreviation for poly(3,4-ethylenedioxythiophene) polystyrene sulfonate and PET is poly(ethylene terephthalate). After fabrication, the final stack is cut to small solar cells with a photoactive area of 1 cm^2.

Standard means to characterize the performance of solar cells include measuring the current density vs. voltage (J-V) curves and the external quantum efficiency (EQE) spectra. For both **P3HT:O-IDTBR** and **P3HT:EH-IDTBR**, the results are shown in **Figure 3** and **Table 1**. The low 2.2% PCE of the **P3HT:EH-IDTBR** solar cell is due to its lower short circuit current (J_{SC}), which is partially limited by the series resistance (Rs) of 9.0 $\Omega \cdot cm^2$ compared to that of P3HT:O-IDTBR of 7.7 .0 $\Omega \cdot cm^2$. The open-circuit voltage (V_{OC}), is similar in both devices (**Table 1**), which reflects the electronic similarity of the two acceptors. The photovoltaic band-gap of the **P3HT:O-IDTBR** and **P3HT:EH-IDTBR** solar cells are 1.60 eV and 1.72 eV, respectively, in agreement with the optical properties observed by the redshift in the EQE shown in **Figure 3** and reported by Enrique P. S. J. et al.[13]. Usually, a redshift is due to a more crystalline structure, thus it is expected that **O-IDTBR** possesses a higher degree of crystallinity than **EH-IDTBR** for the specific coating conditions. The improved J_{SC} of the **P3HT:O-IDTBR** solar cell is in part due to its broader spectral absorbance and the device processing improvements. The integrated EQE currents for the **EH-IDTIBR** and **O-IDTBR** based devices are 5.5 and 8.0 mA/cm^2 under 1 sun illumination as shown in **Figure 3**. From the EQE profiles, it can be seen that the 1:1 mass ratio is close to ideal for **P3HT:O-IDTBR** but is not optimal for **P3HT:EH-IDTBR**. The differences in device performance can partially be explained by the presence of pinholes in the **P3HT:EH-IDTBR** film, whereas **P3HT:O-IDTBR** appears smooth as shown in **Figure 4**. The pinholes in the **P3HT:EH-IDTBR** material system are covered by the subsequent PEDOT:PSS layer during the solar cell fabrication, preventing short-circuiting of the devices. Furthermore, the side chains of the acceptors are respectively linear and branched, which causes their solubility to differ, and thus their drying kinetics. One can use a mini roll-to-roll coater to probe the drying kinetics while coating, which mimics the same coating conditions of the solar cell fabrication[17], as first demonstrated in 2015[18].

Here, we present the application of an improved mini roll-to-roll slot-die coating machine to perform in situ GISAXS experiments, to probe the morphology of the drying inks for OPVs with an in-house X-ray source. GISAXS is the preferred method to probe the size, shape, and orientation distributions in or on thin-films[19]. When performing a GISAXS experiment, the scattered X-rays that probe the sample are collected on a 2D detector. The challenging part is to choose the right model to retrieve the desired information from the sample that is being studied. Therefore, prior information regarding the sample structure is essential to choose a suitable model. Such knowledge can be obtained from atomic force microscopy (AFM), transmission

electron microscopy (TEM), or molecular dynamics simulations[7]. Here, we will present why and how to apply the framework of Teubner and Strey[20] to model the data obtained from the in situ GISAXS experiments to retrieve the size distributions of the domains inside the ink for BHJs while drying. There are two benefits of using a mini roll-to-roll coate. First, it mimics the large-scale production 1:1; thus, we are certain the device performance and active layer can be compared directly. Second, by using this method, we are capable of having enough fresh ink in the beam to ensure an in situ experiment with a laboratory X-ray source. The methods to perform and analyze the morphology of thin-films with GISAXS have been rapidly developing over the past decade[18,21–28]. Usually, when performing an in situ GISAXS experiment to probe drying kinetics of the active layer in OPVs, a synchrotron source is needed[18,26,27]. Synchrotron radiation is in general preferred over an in-house X-ray source to perform such an experiment to provide better time resolution and better statistics. However, synchrotrons are not available on a day-to-day basis and cannot be adjusted to fit a production line, therefore an in-house X-ray source can serve as a useful everyday tool for optimizing ink-formulations, coating conditions, and to gain fundamental insight in the physics of drying kinetics. The most significant disadvantage for using an in-house X-ray source is material consumption. As the flux of X-rays is at least five orders of magnitude smaller than at a synchrotron, more material is needed to obtain sufficient statistics. Therefore, this technique is not yet suitable for new material discovery, where only small amounts of materials are accessible. For materials that are cheap and easy to synthesize, which is also a dominant factor for scalability[29], this method will be advantageous over the usage of synchrotrons in the pursuit of closing the efficiency gap for large scale roll-to-roll coated OPVs[10,30].

This article will guide the reader through performing in situ GISAXS experiments to probe drying kinetics of inks applicable for large-scale production of OPVs. An example of data reduction and analysis is presented along with a discussion of various models to interpret the data.

PROTOCOL

This protocol is divided into five subsections. First, a procedure for preparation of inks is presented. Second, the procedure for preparing and performing roll-to-roll slot-die coating is described. Third, a step-by-step guide for performing an in situ GISAXS experiment is presented. Fourth, a procedure for data correction and analysis is outlined. Finally, the results are reported and discussed.

1. Preparation of inks for roll-to-roll coating (Day 1)

1.1. Read the MSDS of the polymers, molecules, and solvents carefully before starting an experiment.

1.2. Place 90 mg of **O-IDTBR** and 90 mg of **P3HT** in a 10 mL vial.

1.3. Dissolve the P3HT:O-IDTBR solids in 4.5 mL of dichlorobenzene:bromoanisole (0.95:0.05) solvent mixture. The final concentration of the ink is then 180 mg / 4.5 mL = 40 mg/mL.

1.4. Place a magnetic stirrer in the solution and seal the vial immediately. Place the sealed vial on a hot plate with a magnetic rotator. Set the rotation at 300 rpm and the hot plate at 60 °C, and leave it stirring for 12 hours.

1.5. Repeat the procedure for ink preparation for **P3HT:EH-IDTBR**.

2. Preparing and performing roll-to-roll slot die coating (Day 2)

2.1. Turn off the rotation and the hot plate. Remove the vials from the hot plate at least 1 hour before using it, to achieve room-temperature of the inks when coating.

2.2. Wind 18 m of PET substrate foil on the feeder roll. Attach the free end of the substrate to the winder roll as shown in **Figure 5**. Start the motor to run the foil 0.2 m to tighten the substrate.

2.3. Set the first hot plate of the roll-to-roll setup at the desired temperature (i.e., 60 °C). Set the second hot plate at 80 °C to ensure that the film is dried when wound onto the winder roll. Wait approximately 15 min for the temperature of the two hot plates to stabilize.

2.4. Load 2.2 mL of ink into a 3 mL syringe. Mount the syringe in the pump. Attach a tube from the syringe to the slot-die coating head.

2.5. Place the coating head close to the end of the first hot plate by adjusting the horizontal translation stage, and place the meniscus guide approximately 5 mm above the substrate.

2.6. Set the syringe pump at the following coating settings: Rate: 0.08 mL/min, the diameter of syringe: 12.7 mm.

2.7. Control the thickness of the active layer d by adjusting the flow rate, f, and the speed of the moving substrate, v, according to this formula:

$$d = \frac{cf}{\rho v w}$$

where w is the width of the film (determined by the meniscus guide), and ρ is the density of the materials in the ink. In this experiment, we use v=0.6 m/min with a flow rate of f=0.08 mL/min, resulting in a film with a dry thickness of 425 nm.

2.8. **Critical step:** Manually press the ink from the syringe through the hose and stop 1 cm before the ink reaches the coating head. Set the height of the meniscus-guide initially set to 5 mm. Start the syringe pump and wait for a droplet to wet the entire width of the meniscus-guide. Immediately, lower the coating head to wet the substrate with the ink and then raise the meniscus guide to the coating position 2 mm above the substrate.

2.9. Start the motor that winds up the substrate and start coating the ink.

2.10. To stop coating, stop the pump and stop the moving substrate. Raise the coating head to a safe height (approx. 20 mm above the substrate). Then clean the head and hose with tetrahydrofuran.

3. Day 2: In situ roll-to-roll GISAXS experiments

3.1. X-ray setup description

NOTE: The total length of the Grazing Incidence Small Angle X-ray setup is 4.5 m and consists of an X-ray source, focusing optics, a collimation section, a sample stage, a flight tube, beam stop, and a detector, as shown in **Figure 6**. The X-ray source is a rotating anode from Rigaku.

3.1.1. Use a copper anode for this experiment and set the operating condition to 36 kV and 36 mA.

3.1.2. Operate the experiment in fine-focus-mode. The optics consist of a 2D focusing multilayer monochromator, which is aligned to optimize the reflection of the Copper K_α radiation with a wavelength of 1.5418 Å. The collimation section consists of three pinholes placed 45 cm, 141 cm, and 207 cm downstream from the X-ray source, respectively. The diameters of the pinholes are 0.75 mm, 0.3 mm, and 1.0 mm in diameter, respectively, with a probe size of approximately 1.0 mm at the sample position, corresponding to a beam footprint of 286 mm at 0.2° incidence angle. The beam has a flux at the sample of 5 x 10^6 photons s^{-1} and a profile as shown in **Figure 7**, left panel.

3.1.3. Ensure that there are at least three controllable motors at the sample stage to adjust the position of the mini roll-to-roll coater. Downstream of the sample stage, install a 166 cm evacuated flight tube (less than 0.01 mbar) on the rack followed by an Eiger 4M X-ray detector[31].

3.2. Install the roll coater.

3.2.1. Fasten the mini roll-to-roll coater to the goniometer. Mount the goniometer with the roll-to-roll coater on the optical bench at the sample position.

3.2.2. Fasten the three motor cables. Fasten the goniometer stage to the bench. Approach the flight tube as close to the mini roll-to-roll coater as possible.

3.3. **Critical step:** Align the sample position. Coat 10 cm of the ink and roll the film into the beam. The procedure for alignment is threefold.

3.3.1. Align the sample parallel to the beam. This is achieved by an iterative process of scanning the summed intensity of the direct beam as a function of the vertical sample position and incidence angle.

3.3.2. Align the sample to a specific incidence angle, α_i, by calculating the angle from the reflected beam on the detector with the following formula:

$$\boldsymbol{\alpha_i = \frac{1}{2}\arctan\left(\frac{RB[cm] - DB[cm]}{SDD\ [cm]}\right)} \quad \textbf{(1)}$$

where RB is the reflected beam position, DB is the direct beam position (both measured in cm), and SDD is the sample-to-detector distance, here 166 cm.

3.3.3. Optimize the intensity in the reflected beam by scanning the height of the sample position. For this experiment, use an incidence angle of 0.2°. The 2D data for this procedure is shown in **Figure 7**.

3.4. Choice of incidence angle

3.4.1. Choose the angle of incidence to ensure penetration in the layers of interest. Here this will be an incidence angle of 0.2°.

NOTE: For this experiment, the film of interest consists of solvent, P3HT and IDTBR. Both P3HT and O-IDTBR have a higher density than the solvent, and presumably has the highest critical angle for total reflection. The critical angle of P3HT and O-IDBTR can vary according to their packing resulting in a critical angle varying from 0.16° - 0.19°, assuming a density of the solid of 1.1 - 1.35 g/cm^3. Thus, 0.2° was chosen to ensure penetration into the bulk of the film. To perform a GISAXS experiment on another sample system, evaluate the best-suited incidence angle for a specific sample[28,59].

3.5. Install the beam-stop just before the detector, which will extend the lifetime of the detector. Use a circular beam stop for the direct beam and an additional thin rectangular beam stop to block the reflected beam. The beam stop needs to block the direct beam but at the same time allow detection of scattering at low scattering angles.

NOTE: It is possible to perform this experiment without a beam-stop to allow constant tracking of the reflected beam.

3.6. Install the point-suction. Place the point-suction to remove all the gases from the evaporating solvents. Fasten the point-suction to ensure the airflow at the sample is the same at each experiment.

3.7. Load a syringe with 2.2 mL of ink and place the syringe in the syringe pump. Manually press the ink from the syringe through the hose and stop 1 cm before the ink reaches the coating head.

3.8. Set the distance from the coating head to the X-ray beam. Place the coating head at a position of 120 mm displaced from the X-ray beam along the moving direction of the foil, to

ensure a drying time of 12 seconds (for 3 seconds of drying time, place the coating head 30 mm from the X-ray beam) as shown in **Figure 8**.

3.9. Start roll-to-roll slot-die coating. Place the height of the meniscus-guide 5 mm above the substrate.

3.9.1. Start the syringe pump and wait for a droplet to wet the entire width of the meniscus-guide. Immediately, lower the coating head to wet the substrate with ink, and then raise the meniscus guide to the coating position 2 mm above the substrate.

3.9.2. Start the motor that winds up the substrate and start coating the ink.

3.10. Start recording data. Open the X-ray shutter and start recording data for 3000 seconds.

NOTE: This experiment was done with an exposure of 3000 seconds, a more robust method is to perform several shorter exposures to allow flexible temporal binning of data**.**

3.11. Monitor the quality of the coated film with a camera. Look for de-wetting effects of the film on the substrate and meniscus misalignments. If necessary, stop the measurements and redo the experiment.

3.11.1. At the end of experiment, close the X-ray shutter. Turn off the X-ray beam remotely. Stop the syringe pump, raise the coating head and unwind the foil. For a series of experiments, repeat this procedure with a different setting.

4. Data treatment

NOTE: Four experiments were performed and the specific parameters can be found in **Table 2**. One of the experiments with **P3HT:O-IDTBR** was stopped after 2732 seconds due to a syringe pump error; therefore, the signal must be normalized to account for the difference in acquisition time.

4.1. Data correction

4.1.1. First, use a mask to correct for the beam stop and dead pixels[33]. Follow with a cosmic ray filter develop by SAXSLAB, then flat field correction, time correction, a filter for the additional scattering peaks arising from polycrystalline aluminum that are clearly visible in the two datasets shown in **Figure 9**, left panel.

4.2. From real to reciprocal space

4.2.1. Convert the 2D data from real space to the reciprocal space vector $\mathbf{q}_{x,y,z}$ in units of $Å^{-1}$ by using this formula:

$$\boldsymbol{q_{x,y,z}} = \frac{\boldsymbol{2\pi}}{\boldsymbol{\lambda}} \begin{bmatrix} \boldsymbol{\cos(\alpha_f)\cos(2\theta_f) - \cos(\alpha_i)} \\ \boldsymbol{\cos(\alpha_f)\sin(2\theta_f)} \\ \boldsymbol{\sin(\alpha_f) + \sin(\alpha_i)} \end{bmatrix} \quad (2)$$

Here, α_i is the incidence angle with respect to the normal of the surface, α_f is the exit/final angle on the detector (vertical on the detector), $2\theta_f$ is the exit/final angle in the plane (horizontal on the detector), and λ is the wavelength of the incident beam. Assume the wavelength to be preserved, also known as elastic scattering[34].

4.3. Horizontal line integration at the Yoneda line

4.3.1. Determine the *x* and *y* coordinate for the center of the beam, respectively, the sample to detector distance (SDD = 1.66 m), the wavelength of the X-rays (1.5418 Å), and pixel size in each direction (75 x 75 µm^2).

4.3.2. Calculate the expected position of the Yoneda line from the critical angle of the investigated sample[28,34–36].

4.3.3. Retrieve the scattering intensity as a function of scattering vector $\mathbf{q_{xy}}$, by using a MatLab script or by using dedicated software such as DPDAK or Xi-Cam[38,39]. Perform horizontal line integration as indicated in **Figure 9**, with a width of 50 pixels to each side to ensure a satisfying signal-to-noise ratio.

4.4. Binning of horizontal integration

4.4.1. To avoid oversampling (see **Figure 9**, right panel) and to increase the signal-to-noise ratio for the large scattering vectors $\mathbf{q_{xy}}$, bin the data logarithmically[40].

4.4.2. Do not bin the data points up until $\mathbf{q}_{xy} = 0.5 \times 10^{-3}$Å. This is not necessary due to the high intensity and mutual distance in **q**-space, which ensures that there are no redundant data points.

4.4.3. From $\mathbf{q}_{xy} = 0.5 \times 10^{-3}$Å and above, divide the $\mathbf{q_{xy}}$ -axis into 135 equally spaced bins on a logarithmic scale, in such a manner that the first bin at $\mathbf{q}_{xy} = 0.53 \times 10^{-3}$Å is the mean of two data points, and the final binned point at $\mathbf{q}_{xy} = 0.3$ Å is a mean of 24 points.

4.5. Applying the Teubner-Strey model

4.5.1. Apply three Teubner-Strey contributions to describe the data. The first two contributions describe the contrast between the donor/acceptor and the last contribution describes the contrast between larger aggregates of materials surrounded by the solvent. The mathematical expression of the scattering intensity is as follows:

$$\mathbf{I}(q_{xy}) \propto \sum_{\mathbf{i=1}}^{\mathbf{3}} \frac{\mathbf{1}}{\mathbf{a_{1,i}} + \mathbf{c_{1,i}} q_{xy}{}^{\mathbf{2}} + \mathbf{c_{2,i}} q_{xy}{}^{\mathbf{4}}} + \boldsymbol{\beta} \quad (3)$$

where β is a constant background, the parameters $a_{1,i}, c_{1,i}, c_{2,i}$ are defined in terms of the domain size, d_i, and correlation length ξ_i, as follows:

$$\mathbf{a_{1,i}} = \left[\mathbf{1} + \left(\frac{\mathbf{2\pi d_i}}{\boldsymbol{\xi}_\mathbf{i}}\right)^{\mathbf{2}}\right]^{\mathbf{2}},\ \mathbf{c_{1,i}} = -\mathbf{2}\boldsymbol{\xi}_\mathbf{i}^{\mathbf{2}}\left(\frac{\mathbf{2\pi d_i}}{\boldsymbol{\xi}_\mathbf{i}}\right)^{\mathbf{2}} + \mathbf{2}\boldsymbol{\xi}_\mathbf{i}^{\mathbf{2}},\ \mathbf{c_{2,i}} = \boldsymbol{\xi}_\mathbf{i}^{\mathbf{4}} \quad (4)$$

From equations (4), the domain size and correlation length can be expressed as follows:

$$\mathbf{d_i} = \mathbf{2\pi}\left[\frac{\mathbf{1}}{\mathbf{2}}\left(\frac{\mathbf{a_{1,i}}}{\mathbf{c_{2,i}}}\right)^{\mathbf{1/2}} - \frac{\mathbf{1}}{\mathbf{4}}\frac{\mathbf{c_{1,i}}}{\mathbf{c_{2,i}}}\right]^{\mathbf{-1/2}} \quad (5)$$

and

$$\boldsymbol{\xi}_\mathbf{i} = \left[\frac{\mathbf{1}}{\mathbf{2}}\left(\frac{\mathbf{a_{1,i}}}{\mathbf{c_{2,i}}}\right)^{\mathbf{1/2}} + \frac{\mathbf{1}}{\mathbf{4}}\frac{\mathbf{c_{1,i}}}{\mathbf{c_{2,i}}}\right]^{\mathbf{-1/2}} \quad (6)$$

where d_1, ξ_1, d_2 and $\xi_2$are the parameters for the donor/acceptor phases, and d_3 and ξ_3 are the parameters for the aggregate/solvent phases. The fitted models are shown in **Figure 10**. The results from the four fits, based on the described Teubner-Strey model, are found in Table 3.

REPRESENTATIVE RESULTS

First and foremost, this paper describes the method and protocol for performing a successful roll-to-roll in situ in-house GISAXS experiment to probe drying thin-films. Based on the fitting, it can be deduced that the Teubner-Strey model successfully describes the data for P3HT:EH-IDTBR and P3HT:O-IDTBR for both 12 and 3 seconds of drying as shown in **Figure 10**.

The characteristic length scales based on the Teubner-Strey model can be found in **Table 3** with the corresponding errors in **Table 4**. For all four fits, the domain size and correlation length for the highest $\mathbf{q_{xy}}$, d_1 and ξ_1, are close to the same value, varying from 12.0 ± 1.7 nm to 12.5 ± 2.2 nm and from 3.9 ± 0.4 nm to 5.0 ± 0.4nm. These two characteristic sizes and lengths are similar to the values reported in literature for the dry film bulk heterojunctions of P3HT:IDTBR and P3HT:PCBM [41, 42]. For the large structures, d_3 and ξ_3, there is a clear tendency for the structures to become larger as it dries. For P3HT:EH-IDTBR it increases from 225 ± 10.3 nm to 562 ± 11.1 nm, and for P3HT:O-IDTBR it increases from 241 ± 4.1 nm to 489 ± 9.2 nm. The correlation lengths, d_2, are found to 30 ± 12 nm and 34 ± 3.5 nm for P3HT:O-IDTBR and 41 ± 14 nm for

bothP3HT:EH-IDTBR. Noticeably, d_2 is more pronounced after 3 seconds of drying than after 12 seconds of drying for P3HT:O.IDTBR as opposed to P3HT:EH-IDTBR, where the d_2 is more pronounced after 12 seconds of drying than after 3 seconds of drying. Whether d_2 dissolves to contribute to the signal obtained at d_1 or cluster to contribute to d_3 is not determined in this experiment.

Based on the formalism by Teubner-Strey[20], the characteristic parameters for $a_{1,i}, c_{1,i}, c_{2,i}$ indicate that small length scales, $a_{1,1}, c_{1,1}, c_{2,1}$, $a_{1,2}, c_{1,2}, c_{2,2}$, are characteristic for an early stage of spinodal decomposition where the two phases are intermixing[43]. This is in agreement with the general understanding of the morphology of donor/acceptor intermixing. The large length scales, $a_{1,3}, c_{1,3}, c_{2,3}$, are characteristic of micro emulsions[20], which is caused by the contrast (electron density difference) between aggregates of material and solvent. From this experiment, it is impossible to distinguish whether these characteristic parameters of d_3 are caused by the electron density difference between either P3HT:O-IDTBR/Solvent, O-IDTBR/Solvent, or P3HT/Solvent.

To fit a model to X-ray, scattering data is an inherent inverse problem. Therefore, several models can be applied to describe the scattering data. For this analysis, the formulation by Teubner and Strey[20,44] was applied to fit the data. The framework originates from an order parameter expansion of the Landau free energy to describe the scattering intensity from two-phase systems. Interpretation of the model is an abstract geometrical structure of a two-phase system with a characteristic domain size and a correlation length as known from statistical mechanics[45].

There exist many sophisticated models that can predict the 2D data from GISAXS experiments, and user-friendly software programs[34,46] to model this. Usually, GISAXS data from BHJ are modelled with the Distorted Wave Born Approximation (DWBA) with very high accuracy[27,40,47,48]. Nevertheless, the main disadvantage is that the modelled structure is not corresponding to the complexity expected in a BHJ. A simpler approach is to restrict the analysis to the $\mathbf{q_{xy}}$ direction. When only 1D horizontal line cuts in $\mathbf{q_{xy}}$ are considered, it is fair to assume that the main contributor to scattering arises from the lateral structures present in the film. Assuming this it can be shown that the momentum transfer retrieved from the horizontal line cuts corresponds to transmission SAXS[49,50], from where Teubner-Strey is derived[20] and therefore valid for the analysis presented here.

This model is chosen for three reasons: First, the model is an analytical expression that has been proved to fit a variety of two-phase systems including BHJ[20,26,51], and it can be employed for very fast fitting algorithms, which is applicable for large-scale quality control and for in situ measurements. Second, to the best of our knowledge, this model is in agreement with the morphology observed for P3HT:O-IDTBR by transmission electron microscopy (TEM)[52] and atomic force microscopy (AFM)[42]. Third, it is a simple model i.e. it spans a small parameter space.

Furthermore, this paper documents that probing drying kinetics of non-fullerene organic solar cells with an in-house X-ray source is possible. In addition, this method has the potential to serve as a tool for accelerating the research in large-scale roll-to-roll coated OPVs.

Figure 1: Chemical structure of P3HT, O-IDTBR, and EH-IDTBR.

Figure 2: (Left) Working principle of a bulk heterojunction organic solar cell. Sunlight is creating an exciton, which upon separation allows the hole and the electron to diffuse to the cathode and anode, respectively. (Right) Energy diagram of the HOMO and LUMO levels of the donor and acceptor.

Figure 3: (Left) JV-curves for roll slot die coated on flexible substrate P3HT:O-IDTBR and P3HT:EH-IDTBR, corresponding to the best performing devices shown in Table 1. (Right) EQE curves of roll slot die coated on flexible substrate P3HT:O-IDTBR and P3HT:EH-IDTBR.

Figure 4: Images of the two inks, roll coated on PET substrate. Top is P3HT:EH-IDTBR and bottom is P3HT:O-IDTBR.

Figure 5: (Left) Image of micro roll-to-roll coater. 1. a) 1.b) are indicating the rotation centre of the foil feeder and receiver, respectively. The motor is on the backside of the roll-to-roll coater and is a stepper motor. 2) The translation stages for the coating head, which can move in all three directions, along the foil, up and down, and outwards and inwards. 3) The slot die coating head, where a hose with ink can be fastened. 4) The two hot plates, indicated by the two arrows, which will heat the moving substrate to the desired temperature. In this experiment, it was set to 65 °C. All parts are controlled remotely. (Right) Roll-to-roll coater installed at the GISAXS set-up.

Figure 6: Experimental set-up for Grazing Incidence Small Angle X-ray Scattering. 1) X-ray source is a rotating anode made by Rigaku. A rotating anode made from copper was operated at 36 kV 36 mA. 2) Optics section, where the Cu K_α characteristic fluorescence from the rotating anode diffract from a single bounce multilayer mirror, which makes the beam monochromatic at wavelength: λ=1.5418 Å. 3) Attenuator station, which was not applied for this experiment. 4) Collimation section, consisting of three pinholes after each other as indicated with the three arrows. The diameter of the pin holes are 0.75 mm, 0.3 mm, and 1.0 mm, respectively. 5) Mini roll-to-roll coater position attached to a vertical moving axis and a goniometer to control the incidence angle. 6) Flight tube in vacuum. 7) Eiger 4M detector.

Figure 7: Three steps in the alignment procedure illustrated as raw Eiger 4M data. (Left) First, make sure there is nothing blocking the direct beam. In this example the beam stop is located just to the left and beneath the direct beam. (Middle) Scan the sample along the vertical axis and place it where half of the direct beam is blocked by the sample. Then rotate the sample to gradually changing the incidence angle and place the sample where the intensity of the direct beam is highest. This procedure must be done 3-5 times to ensure that the sample is completely parallel with the beam. (Right) Rotate the sample until a clear reflection occur on the detector. From these two positions, the exact incident angle can be calculated (see text).

Figure 8: Two stages of drying seen from two different angles. (Left) is the **wet** stage, where the film has been drying for 3 seconds before being probed. (Right) is the **dry stage** where the film

has been drying for 12 seconds. The contrast have been increased to visualize the effect of the edges drying.

Figure 9: (Left) 2D data P3HT:O-IDTBR at 12 seconds of drying with 3000 seconds of acquisition time. The red rectangle indicates where the horizontal integration has been performed and the intense areas marked as aluminum peaks originates from the heater plate. (Right) The horizontal integration from the red rectangle where the q-vectors of the aluminum peaks are omitted from the integration.

Figure 10: Binned horizontal line integration for the four experiments: P3HT:EH-IDTBR (black) and P3HT:O-IDTBR (blue) probed at both 12 seconds (triangles) and 3 seconds (squares) of drying along with the Teubner-Strey fits.

Table 1: Optoelectronic characteristics of 1 cm^2 organic solar cells based in P3HT:O-IDTBR and P3HT:EH-IDTBR showing the power conversion efficiency (PCE), the short circuit current density (J_{SC}), the fill factor (FF), and the open circuit voltage (V_{OC}), under 100 mW/cm^2 illumination.

Table 2: Overview of data. P3HT:O-IDTBR with a drying time of 3.0 s was stopped after 2732 s due to a syringe pump error.

Table 3: Fitted values from the four experiments. All units of [nm].

Table 4: Errors of the fitted values from the four experiments. All units of [nm].

DISCUSSION

The incidence angle is very important for a GISAXS experiment. It can be questioned how stable the film will move with respect to the incident angle during roll-to-roll coating of 18 meters film on a flexible substrate. For the experiments performed in this demonstration, we cannot prove the stability of the moving substrate, but previous published data where an older version of the setup is used, document a stable film[18,21]. Previous synchrotron experiments where this roll-to-roll coater has been used have demonstrated that the incidence angle does not vary more than ± 0.03° as evaluated by the position of the reflected beam as a function of time (with a temporal resolution of 0.1 s), which is equal to ± 12 pixels from the Yoneda line for this experiment, whereas, the horizontal line integration were made with ± 50 pixels. Under the assumption made for this analysis, this small change of incidence angle will not influence the analysis of this work and can therefore be neglected. In the future, this type of experiments should be performed without a beam-stop and with continuous collection of data to probe the angle of incidence throughout the experiment.

Air convection above the drying film, relative pressure, and relative humidity are known to influence the drying-profile of thin-films; thus, to make a fully reproducible experiment, carefully measuring these parameters is a necessity. Comparison between the four measurements in this paper is valid due to the fact that these were coated under the exact same conditions on the same day.

To perform a roll-to-roll in situ GISAXS experiment, several criteria must be fulfilled to ensure a successful experiment. The differences in electron density (contrast) between the materials need to be high enough in order to have a scattering signal. Guidelines on this topic have been published J. Als-Nielsen et al.[53].

Due to the low X-ray flux of a laboratory source relative to a synchrotron, much more material is needed to perform such experiments. Thus, it is not fully applicable for materials discovery but will serve as a tool for optimization of formulations of inks relevant for OPVs. Additionally to the low flux, it is only possible to perform coarser experiments with respect to the temporal resolution of drying inks. During such experiments we are probing 18 meters of active layer while drying. We expect small variations in the large-scale morphology throughout the experiment, and we therefore probe the mean of 18 meters of coated film. This mimics the conditions of a large scale fabrication. If the inhomogeneity within a few meters are to be studied, synchrotron radiation is needed.

Performing exposures of 3000 seconds is not the optimal experimental design. A more robust method is to perform several shorter exposures to allow flexible temporal binning of data to analyze the large scale homogeneities and to probe the incidence angle at all times.

To the best of our knowledge, this is the first demonstration of performing an in situ GISAXS on roll-to-roll coating of inks for OPVs on a laboratory X-ray source, although we have previously demonstrated similar experiments analyzing the crystalline diffraction signal[54,55]. With this demonstration and protocol, we believe it will be easier to apply and perform in situ GISAXS experiments for researchers, students, and developing engineers. This can potentially accelerate the research field, simply because it is possible to access such equipment on a day-to-day basis. Additionally, by using a roll-to-roll coater it is possible to compare the solar cell performance with the structural properties probed in this experiment, 1:1.

Improvements of the experimental setup are required to exploit all the advantages of having an in house X-ray source. Besides increasing the usable X-ray flux for small laboratory sources, the first step for the improvement of this experiment is to avoid scattering peaks from aluminum that are overlying the data, as shown in **Figure 9** (left). This can be realized by installing an X-ray absorbing substrate holder that can withstand temperatures up to 150 °C for proper heating. Additionally, guard slits just before the sample will improve the data quality. This demonstration is not exclusively of interest for research in the organic solar cell community, but any field that is researching or optimizing coating parameters for thin-film technologies. Combining this technique with simultaneous GIWAXS, where crystalline structures are probed, will further increase the number of the scientific fields where in house roll-to-roll X-ray experiments are applicable.

As these in situ roll-to-roll experiments are probing wet films, it is beneficial if the solvent is not absorbing too large fractions of the illuminated X-ray beam. In general polymer:PCBM systems have a large contrast and combined with a solvent that does not contain chlorine (which is a

strong X-ray absorber) will guarantee a large contrast, thus a high scattering intensity. For this experiment, the contrast of P3HT:IDTBR is small and combined with a chlorinated solvent the scattering intensity is low. These materials are not ideal for such an experiment, but very interesting for solar cells, which is why this technique must be further developed to ensure that systems with low contrast and high absorbance can be probed as well. The choice of model is the most determining factor to perform a comparative analysis across several GISAXS experiments. For the analysis presented in this paper, the framework of Teubner-Strey was applied to describe the four data sets. The best method to choose a model is to possess ab initio information about the shape and size of the investigated sample. This can be achieved from either TEM images, simulations, or microscope pictures. The reasoning behind our choice of model is stated in the text, but it should be noted that several models can be chosen for describing such GISAXS data. The Teubner-Strey model was originally developed for transmission SAXS but have successfully modelled GIWAXS data of BHJ solar cells before[51] and now here. Further improvements are to adapt abstract geometric models as known from molecular dynamics simulations and apply DWBA to model 2D data. Alternative models include: strict geometrical objects with a degree of polydisperse distribution of size as described and applied in[53], where the DWBA is necessary to model 2D data, a combination of Fresnel reflectivity and Gaussian distributions to fit ordered systems as co-block polymers GISAXS signals[56], bead models mainly for biological samples[57], and fractal geometry[58,59].

ACKNOWLEDGEMENTS

The authors would like to acknowledge the two technicians who helped rebuilding and maintaining the instrument, Kristian Larsen and Mike Wichmann. Furthermore, the authors would like to thank Roar R. Søndergaard and Anders Skovbo Gertsen for fruitful discussions. This study was supported by the European Research Council (ERC) under the European Union's Horizon 2020 research and innovation programme (SEEWHI Consolidator grant No. ERC-2015-CoG-681881).

DISCLOSURES

The authors have nothing to disclose.

REFERENCES

1. Krebs, F.C., Espinosa, N., Hösel, M., Søndergaard, R.R., Jørgensen, M. 25th Anniversary Article: Rise to Power - OPV-Based Solar Parks. *Advanced Materials*. **26** (1), 29–39 (2014).
2. Søndergaard, R., Hösel, M., Angmo, D., Larsen-Olsen, T.T., Krebs, F.C. Roll-to-roll fabrication of polymer solar cells. *Materials Today*. **15** (1–2), 36–49 (2012).
3. Lucera, L. et al. Guidelines for Closing the Efficiency Gap between Hero Solar Cells and Roll-To-Roll Printed Modules. *Energy Technology*. **3** (4), 373–384 (2015).
4. Gu, X. et al. Roll-to-Roll Printed Large-Area All-Polymer Solar Cells with 5% Efficiency Based on a Low Crystallinity Conjugated Polymer Blend. *Advanced Energy Materials*. **7** (14), 1602742 (2017).
5. Ding, Z., Stoichkov, V., Horie, M., Brousseau, E., Kettle, J. Spray coated silver nanowires as transparent electrodes in OPVs for Building Integrated Photovoltaics applications. *Solar Energy Materials and Solar Cells*. **157**, 305–311 (2016).

6. Few, S., Frost, J.M., Nelson, J. Models of charge pair generation in organic solar cells. *Physical Chemistry Chemical Physics*. **17** (4), 2311–2325 (2015).
7. Alessandri, R., Uusitalo, J.J., De Vries, A.H., Havenith, R.W.A., Marrink, S.J. Bulk Heterojunction Morphologies with Atomistic Resolution from Coarse-Grain Solvent Evaporation Simulations. *Journal of the American Chemical Society*. **139** (10), 3697–3705 (2017).
8. Mirsafaei, M. et al. The influence of electrical effects on device performance of organic solar cells with nano-structured electrodes. *Scientific Reports*. **7** (1) (2017).
9. Liu, Q. et al. 18% Efficiency organic solar cells. *Science Bulletin* (2020).
10. Gertsen, A.S., Castro, M.F., Søndergaard, R.R., Andreasen, J.W. Scalable fabrication of organic solar cells based on non-fullerene acceptors. *Flexible and Printed Electronics*. **5** (1), 014004 (2020).
11. Holliday, S. et al. High-efficiency and air-stable P3HT-based polymer solar cells with a new non-fullerene acceptor. *Nature Communications*. **7**, 1–11 (2016).
12. Yan, C., Barlow, S., Jen, A.K.-Y., Marder, S. Non-fullerene acceptors for organic solar cells High Energy Density Nanocomposites Based on Surface-Modified BaTiO3 and a Ferroelectric Polymer View project Organic Solar Cells View project. *Nature Publishing Group*. **3**, 1–19 (2018).
13. Pascual-San-José, E. et al. Blade coated P3HT:non-fullerene acceptor solar cells: a high-throughput parameter study with a focus on up-scalability. *Journal of Materials Chemistry A*. **7** (35), 20369–20382 (2019).
14. Strohm, S. et al. P3HT: Non-fullerene acceptor based large area, semi-transparent PV modules with power conversion efficiencies of 5%, processed by industrially scalable methods. *Energy and Environmental Science*. **11** (8), 2225–2234 (2018).
15. Liu, K. et al. Roll-coating fabrication of flexible organic solar cells: comparison of fullerene and fullerene-free systems †. Journal of Materials Chemistry C. (3) (2016).
16. He, Z. et al. Enhanced power-conversion efficiency in polymer solar cells using an inverted device structure. *Nature Photonics*. **6** (9), 591–595 (2012).
17. Andersen, T.R. et al. Scalable, ambient atmosphere roll-to-roll manufacture of encapsulated large area, flexible organic tandem solar cell modules. *Energy and Environmental Science*. **7** (9), 2925–2933 (2014).
18. Rossander, L.H. et al. In-line, roll-to-roll morphology analysis of organic solar cell active layers. *Energy and Environmental Science.* 2411–2419 (2017).
19. Müller-Buschbaum, P. A basic introduction to grazing incidence small-angle X-ray scattering. *Lecture Notes in Physics*. **776**, 61–89 (2009).
20. Teubner, M., Strey, R. Origin of the scattering peak in microemulsions. *The Journal of Chemical Physics*. **87** (5), 3195–3200 (1987).
21. Böttiger, A.P.L., Jorgensen, M., Menzel, A., Krebs, F.C., Andreasen, J.W. High-throughput roll-to-roll X-ray characterization of polymer solar cell active layers. *Journal of Materials Chemistry*. **22** (42), 22501–22509 (2012).
22. Herzog, G. et al. In situ grazing incidence small-angle X-ray scattering investigation of polystyrene nanoparticle spray deposition onto silicon. *Langmuir*. **29** (36), 11260–11266 (2013).
23. Perlich, J. et al. Pattern formation of colloidal suspensions by dip-coating: An in situ

grazing incidence X-ray scattering study. *physica status solidi (RRL) - Rapid Research Letters*. **6** (6), 253–255 (2012).
24. Schwartzkopf, M., Roth, S. Investigating Polymer–Metal Interfaces by Grazing Incidence Small-Angle X-Ray Scattering from Gradients to Real-Time Studies. *Nanomaterials*. **6** (12), 239 (2016).
25. Fan, Q. et al. High-Performance As-Cast Nonfullerene Polymer Solar Cells with Thicker Active Layer and Large Area Exceeding 11% Power Conversion Efficiency. *Advanced Materials*. **30** (6), 1–7 (2018).
26. Liu, F. et al. Fast printing and in situ morphology observation of organic photovoltaics using slot-die coating. *Advanced Materials*. **27** (5), 886–891 (2015).
27. Liu, F. et al. Printing Fabrication of Bulk Heterojunction Solar Cells and In Situ Morphology Characterization. *Journal of Visualized Experiments*. (119), 53710 (2017).
28. Hexemer, A., Müller-Buschbaum, P. Advanced grazing-incidence techniques for modern soft-matter materials analysis. *IUCrJ*. **2** (1), 106–125 (2015).
29. Carlé, J.E., Helgesen, M., Madsen, M. V., Bundgaard, E., Krebs, F.C. Upscaling from single cells to modules-fabrication of vacuum- and ITO-free polymer solar cells on flexible substrates with long lifetime. *Journal of Materials Chemistry C*. **2** (7), 1290–1297 (2014).
30. Carlé, J.E. et al. Overcoming the Scaling Lag for Polymer Solar Cells. *Joule*. **1** (2), 274–289 (2017).
31. Dectris *Technical Specifications EIGER R 4M Detector Systems*. at <www.dectris.com>. (2018).
32. Riekel, C., Burghammer, M., Davies, R., Gebhardt, R., Popov, D. Applications of Synchrotron Light to Scattering and Diffraction in Materials and Life Sciences. *Lecture Notes in Physics*. **776** (2009), 91–104 (2009).
33. Pauw, B.R. Everything SAXS: Small-angle scattering pattern collection and correction. *Journal of Physics Condensed Matter*. **25** (38), 1–2 (2013).
34. Babonneau, D. FitGISAXS: Software package for modelling and analysis of GISAXS data using IGOR Pro. *Journal of Applied Crystallography*. **43** (4), 929–936 (2010).
35. Yoneda, Y. Anomalous surface reflection of X rays. *Physical Review*. **131** (5), 2010–2013 (1963).
36. Schwartzkopf, M., Roth, S. V. Investigating polymer–metal interfaces by grazing incidence small-angle x-ray scattering from gradients to real-time studies. *Nanomaterials*. **6** (12) (2016).
37. Liu, J., Yager, K.G. Unwarping GISAXS data. *IUCrJ*. **5**, 737–752 (2018).
38. Benecke, G. et al. A customizable software for fast reduction and analysis of large X-ray scattering data sets: Applications of the new DPDAK package to small-angle X-ray scattering and grazing-incidence small-angle X-ray scattering. *Journal of Applied Crystallography*. **47** (5), 1797–1803 (2014).
39. Pandolfi, R.J. et al. Xi-cam: a versatile interface for data visualization and analysis. *Journal of Synchrotron Radiation*. **25** (4), 1261–1270 (2018).
40. Pröller, S. et al. Following the Morphology Formation In Situ in Printed Active Layers for Organic Solar Cells. *Advanced Energy Materials*. **6** (1), 1501580 (2016).
41. Pedersen, E.B.L. et al. Structure and crystallinity of water dispersible photoactive nanoparticles for organic solar cells. *Journal of Materials Chemistry A*. **3** (33), 17022–

17031 (2015).
42. Liang, Q. et al. Separating Crystallization Process of P3HT and O-IDTBR to Construct Highly Crystalline Interpenetrating Network with Optimized Vertical Phase Separation. *Advanced Functional Materials*. **29** (47), 1807591 (2019).
43. Allen, S.M. Spinodal Decomposition. *Encyclopedia of Materials: Science and Technology*. 8761–8764 (2001).
44. Schubert, K. V., Strey, R., Kline, S.R., Kaler, E.W. Small angle neutron scattering near Lifshitz lines: Transition from weakly structured mixtures to microemulsions. *The Journal of Chemical Physics*. **101** (6), 5343–5355 (1994).
45. Gould, H., Tobochnik, J. *Statistical and thermal physics : with computer applications*. Princeton University Press. (2010).
46. Pospelov, G. et al. BornAgain: software for simulating and fitting grazing-incidence small-angle scattering. *Journal of Applied Crystallography*. **53**, 262–276 (2020).
47. Wienhold, K.S. et al. Effect of Solvent Additives on the Morphology and Device Performance of Printed Nonfullerene Acceptor Based Organic Solar Cells. *ACS Applied Materials & Interfaces*. 11 (45), 42313-42321 (2019).
48. Pröller, S. et al. Electrophoresis Assisted Printing: A Method to Control the Morphology in Organic Thin Films. *ACS Applied Materials and Interfaces*. **12** (5), 5219–5225 (2020).
49. Busch, P., Rauscher, M., Smilgies, D.M., Posselt, D., Papadakis, C.M. Grazing-incidence small-angle X-ray scattering from thin polymer films with lamellar structures - The scattering cross section in the distorted-wave Born approximation. *Journal of Applied Crystallography*. **39** (3), 433–442 (2006).
50. Busch, P., Posselt, D., Smilgies, D.M., Rauscher, M., Papadakis, C.M. Inner structure of thin films of lamellar poly(styrene-b-butadiene) diblock copolymers as revealed by grazing-incidence small-angle scattering. *Macromolecules*. **40** (3), 630–640 (2007).
51. Kozub, D.R . et al. Polymer Crystallization of Partially Miscible Polythiophene/Fullerene Mixtures Controls Morphology. *Macromolecules*. **44**, 5722–5726 (2011).
52. Köntges, W. et al. Visualizing morphological principles for efficient photocurrent generation in organic non-fullerene acceptor blends. *Energy & Environmental Science*. 1259–1268 (2020).
53. Als-Nielsen, J., McMorrow, D. *Elements of Modern X-ray Physics: Second Edition*. *Elements of Modern X-ray Physics: Second Edition*. John Wiley and Sons. (2011).
54. Rossander, L.H., Zawacka, N.K., Dam, H.F., Krebs, F.C., Andreasen, J.W. In situ monitoring of structure formation in the active layer of polymer solar cells during roll-to-roll coating. *AIP Advances*. **4** (8) (2014).
55. Zawacka, N.K. et al. The influence of additives on the morphology and stability of roll-to-roll processed polymer solar cells studied through ex situ and in situ X-ray scattering. *Journal of Materials Chemistry A*. **2** (43), 18644–18654 (2014).
56. Renaud, G., Lazzari, R., Leroy, F. Probing surface and interface morphology with Grazing Incidence Small Angle X-Ray Scattering. *Surface Science Reports*. **64** (8), 255–380 (2009).
57. Hajizadeh, N.R., Franke, D., Jeffries, C.M., Svergun, D.I. Consensus Bayesian assessment of protein molecular mass from solution X-ray scattering data. *Scientific Reports*. **8** (1) (2018).
58. Bale, H.D., Schmidt, P. *Small-Angle X-Ray-Scattering Investigation of Submicroscopic*

Porosity with Fractal Properties. **3** (6) (1984).
59. Anitas, E.M., Slyamov, A. Structural Properties of Additive Nano/Microcellular Automata. *Annalen der Physik*. **530** (6), 1800004 (2018).

Figure 1

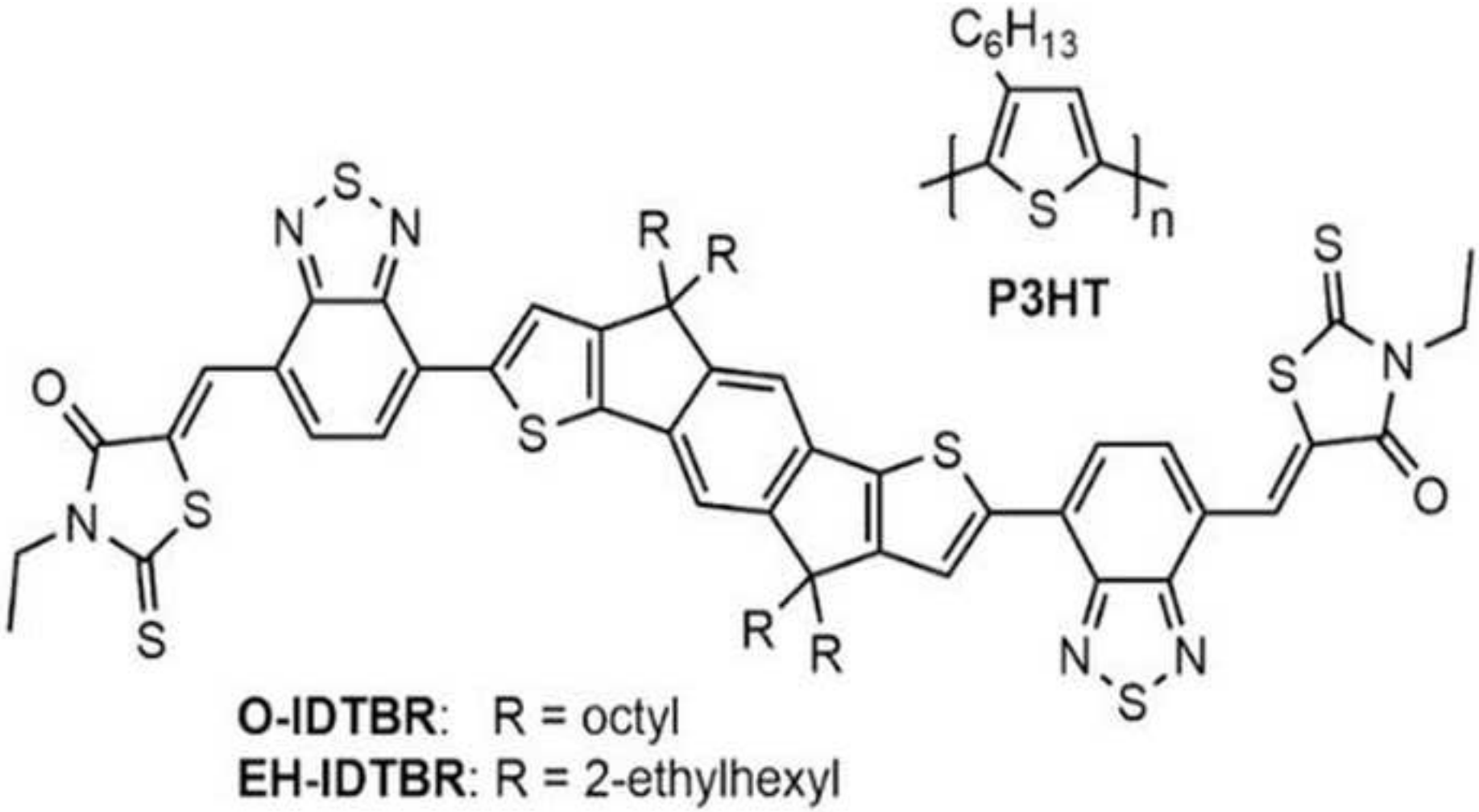

Figure 2

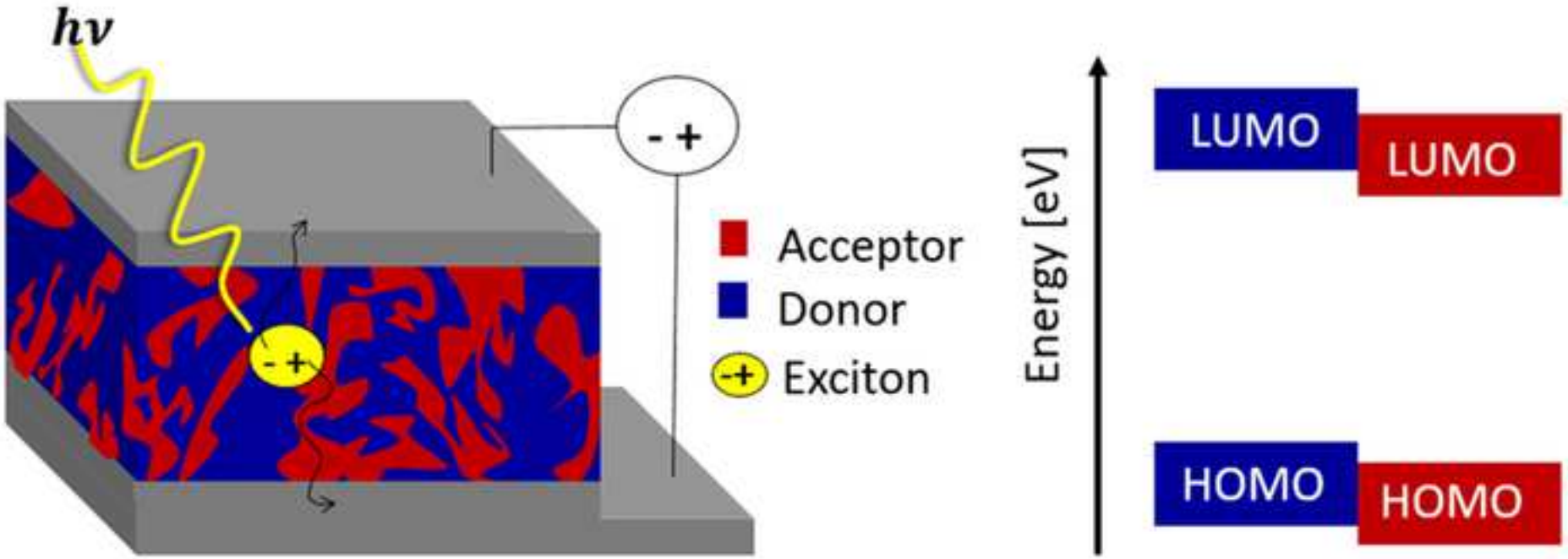

Figure 3

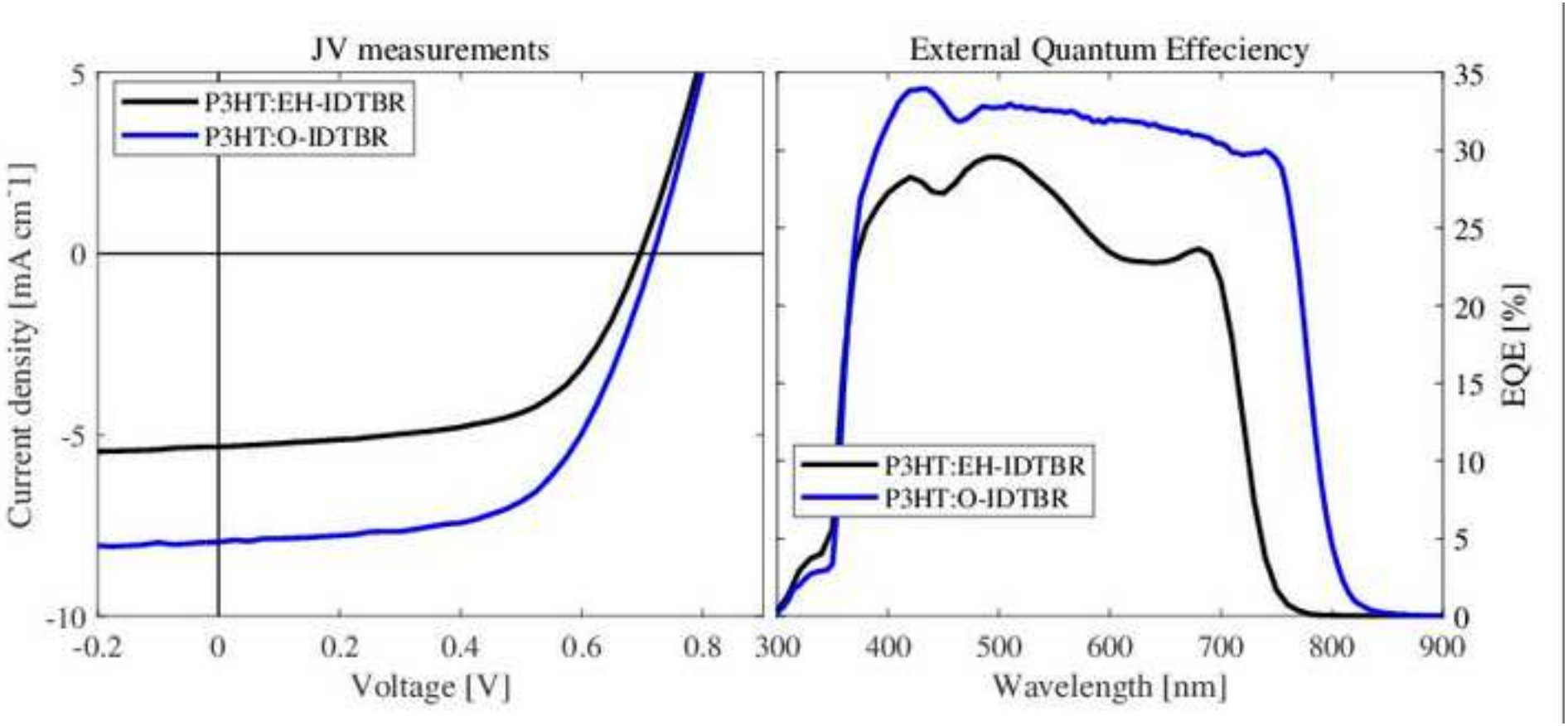

Figure 4

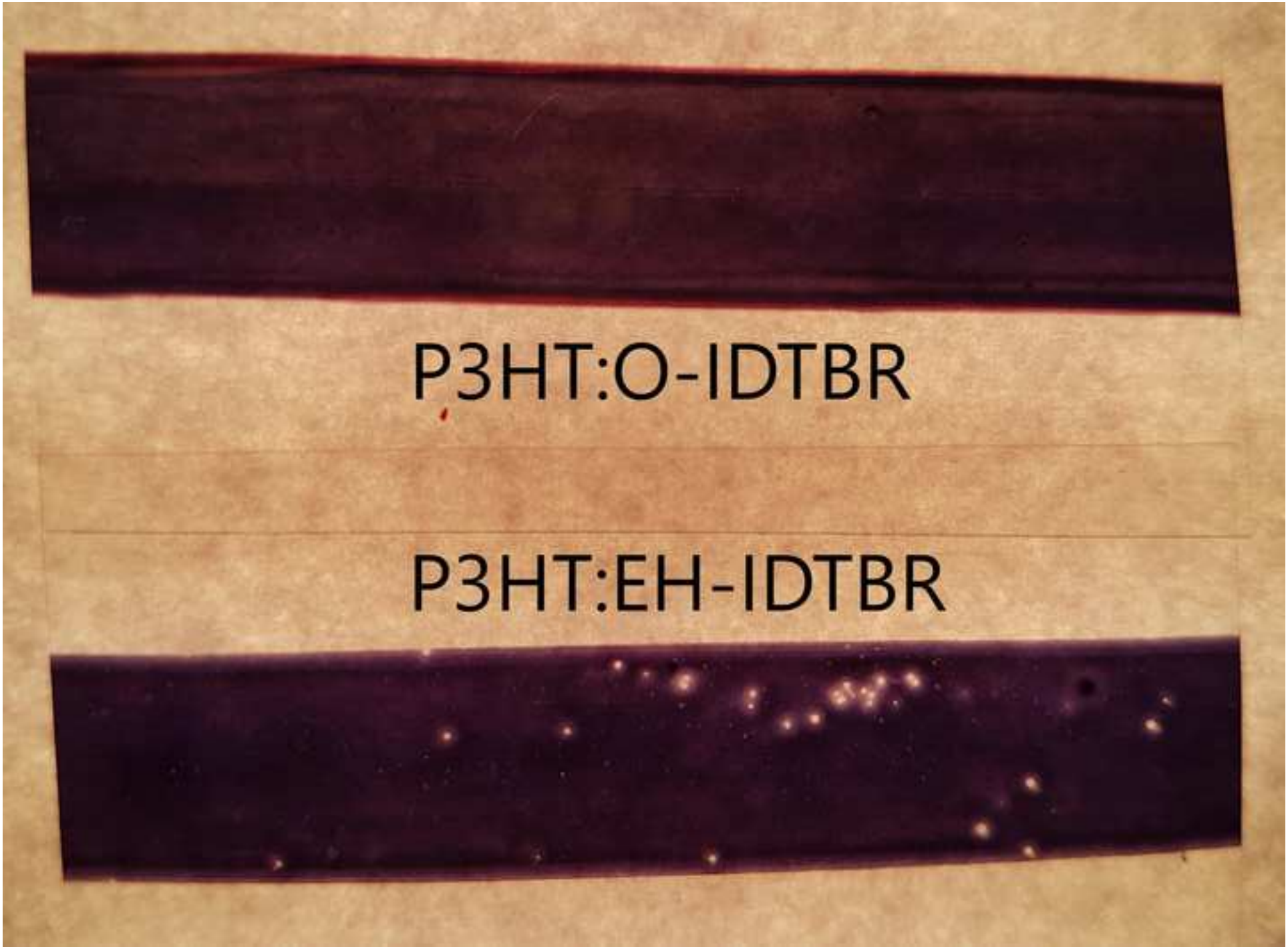

Figure 5a

Click here to access/download;Figure;fig_5_left.jpg

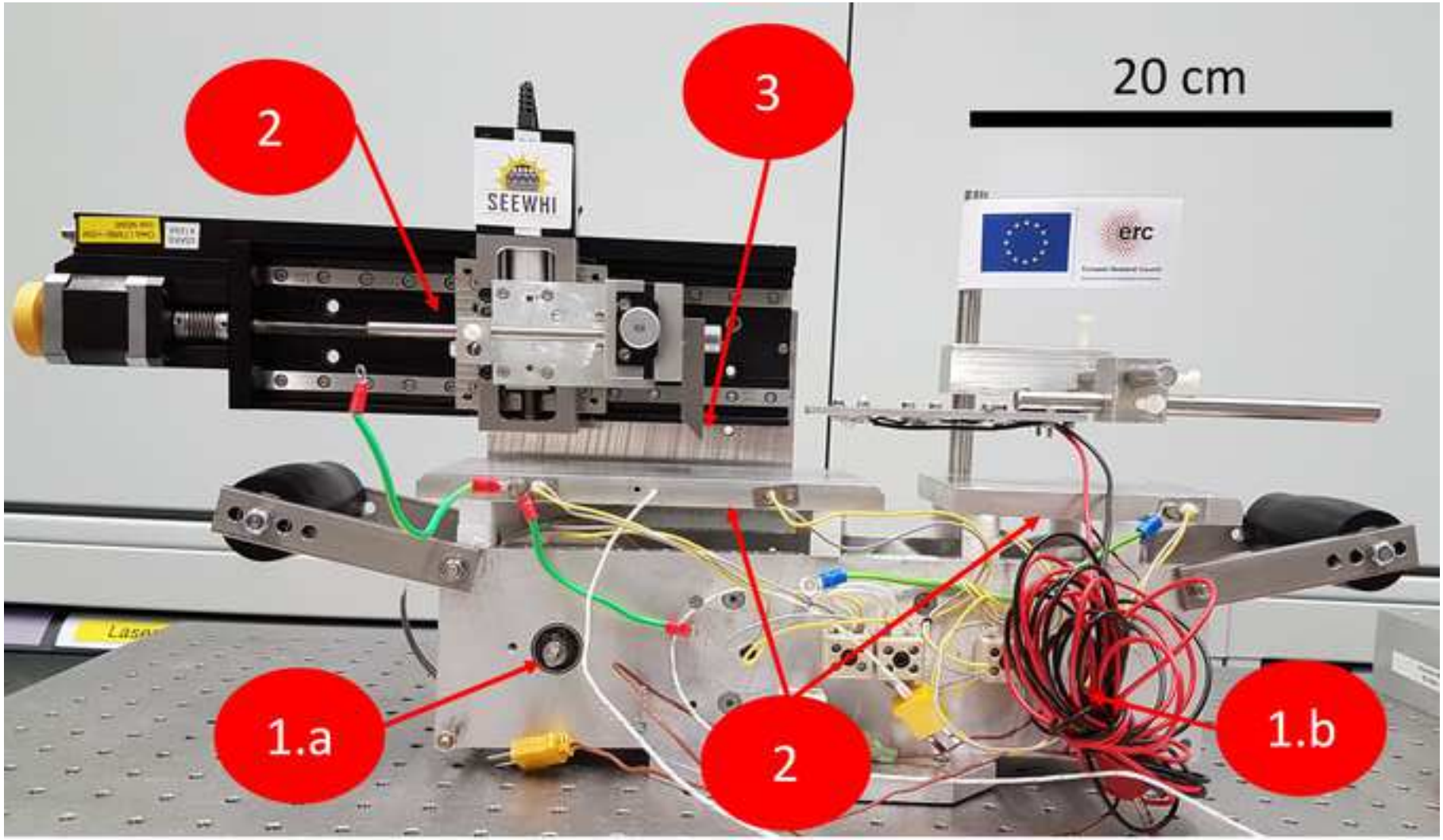

Figure 5b

Click here to access/download;Figure;fig_5_right.jpg

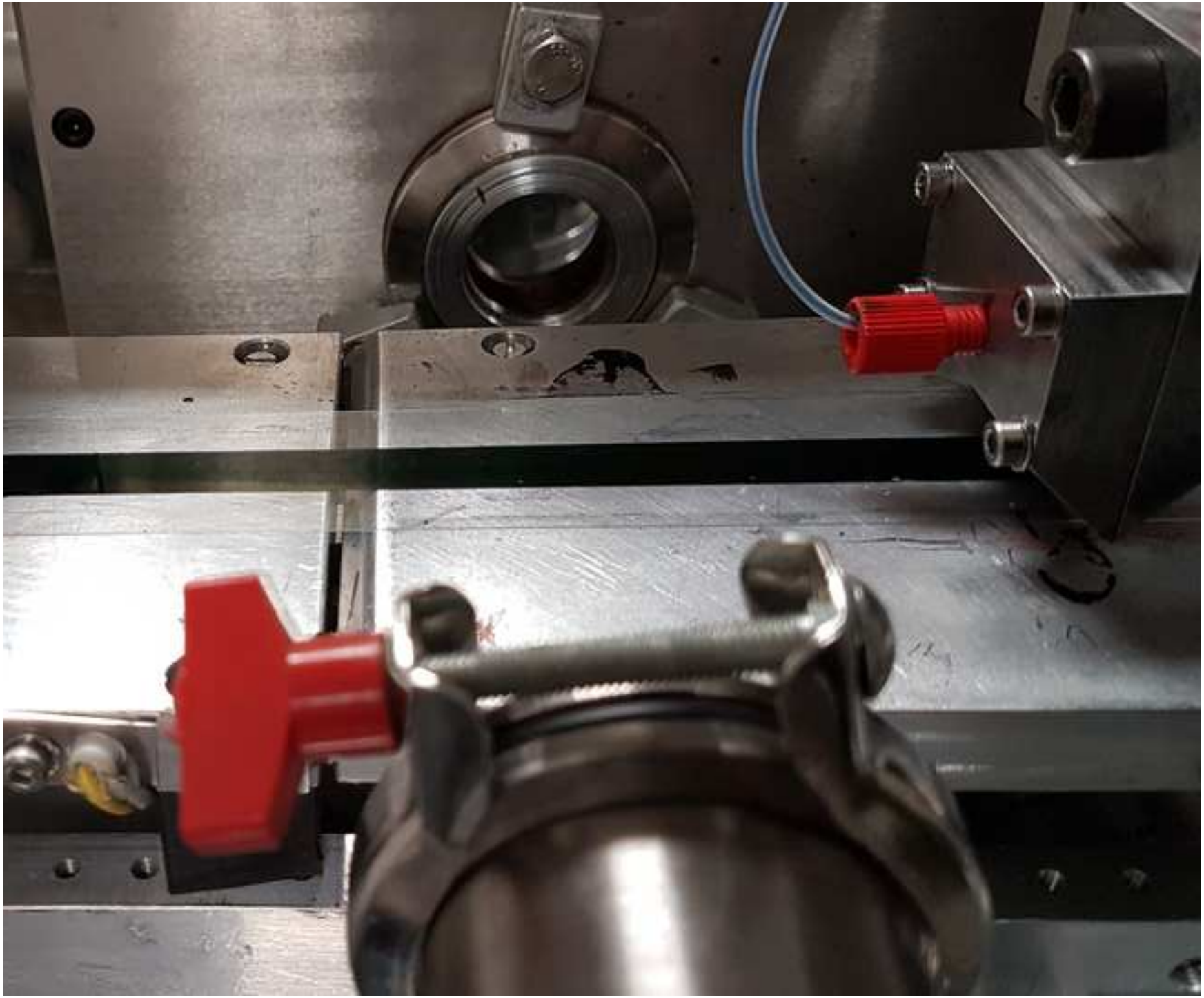

Figure 6

Click here to access/download;Figure;fig_6.png

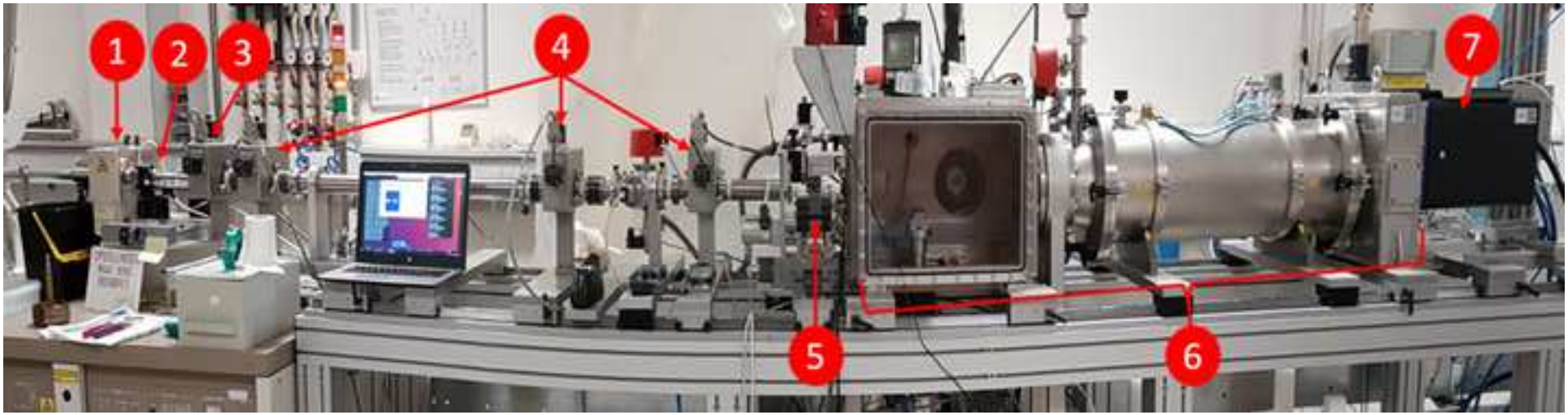

Figure 7

Click here to access/download;Figure;fig_7.png

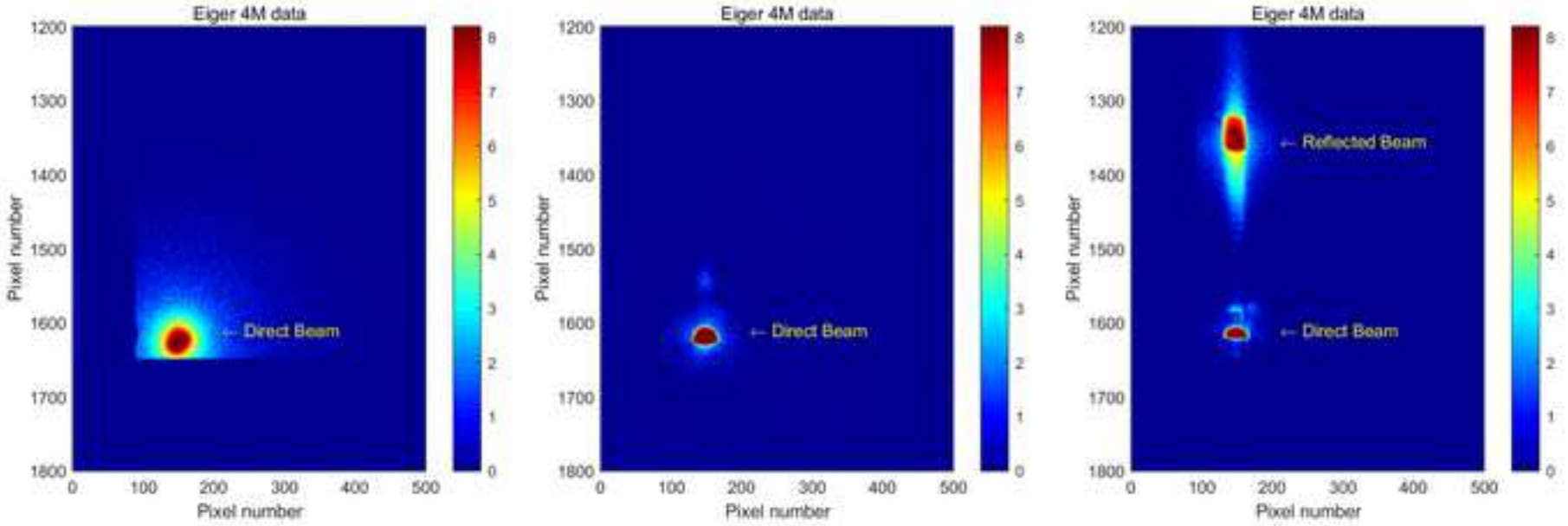

Figure 8

Click here to access/download;Figure;fig_8.png

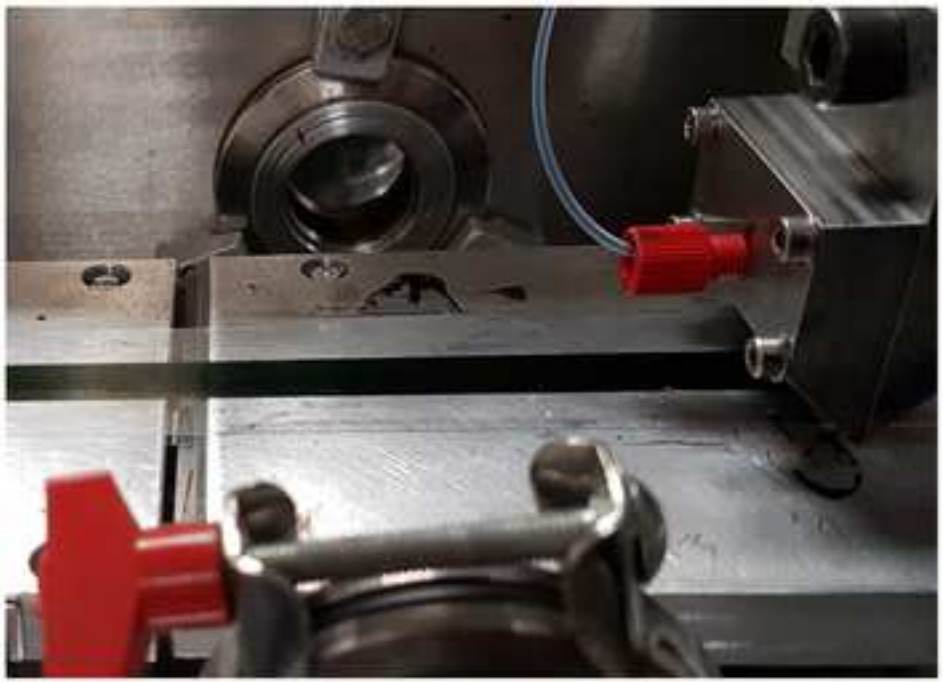

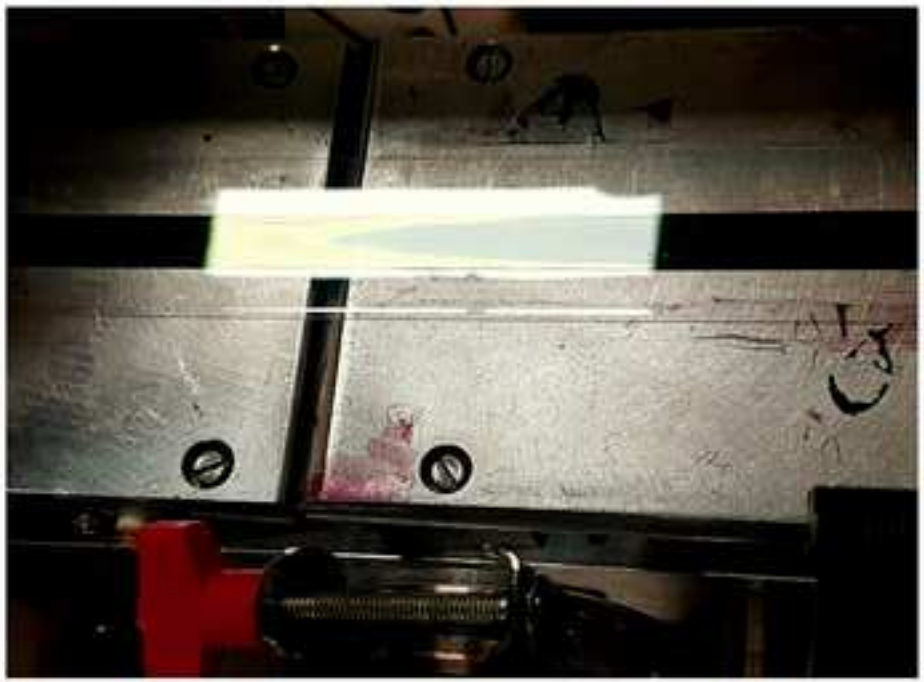

Figure 9a

Click here to access/download;Figure;fig_9left.jpg

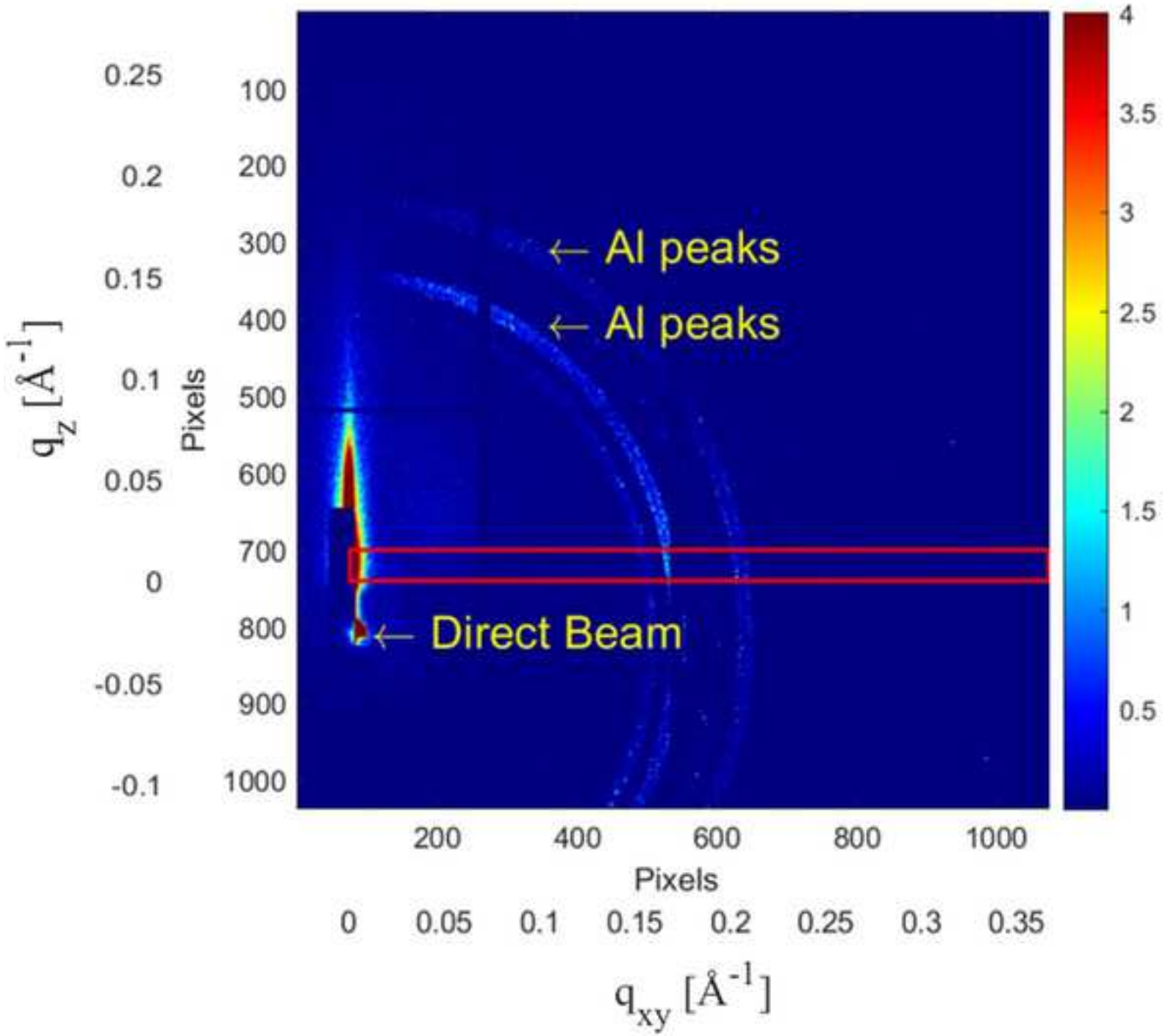

Figure

Click here to access/download;Figure;fig_9_right.jpg

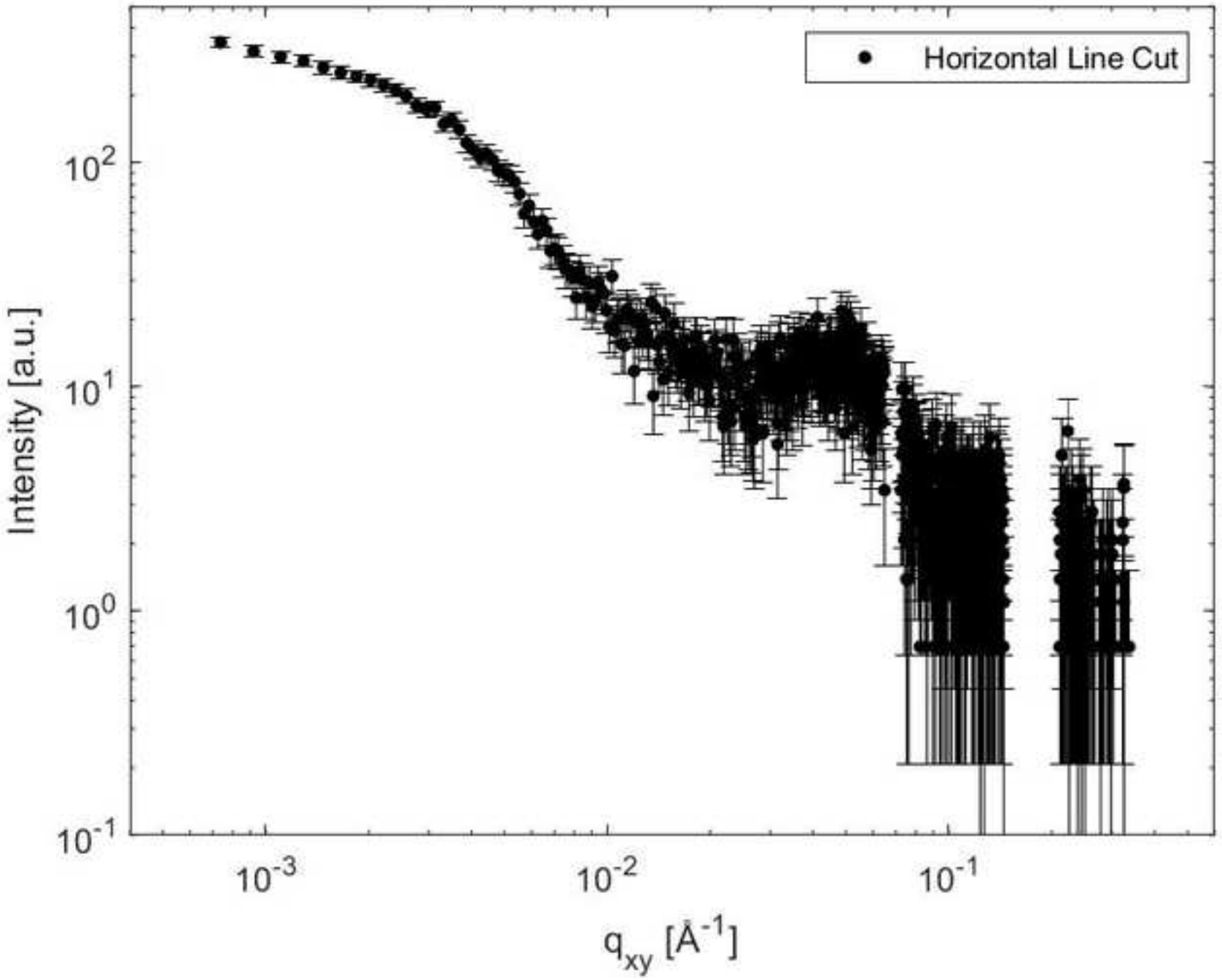

Figure 10

Click here to access/download;Figure;figure10.jpg

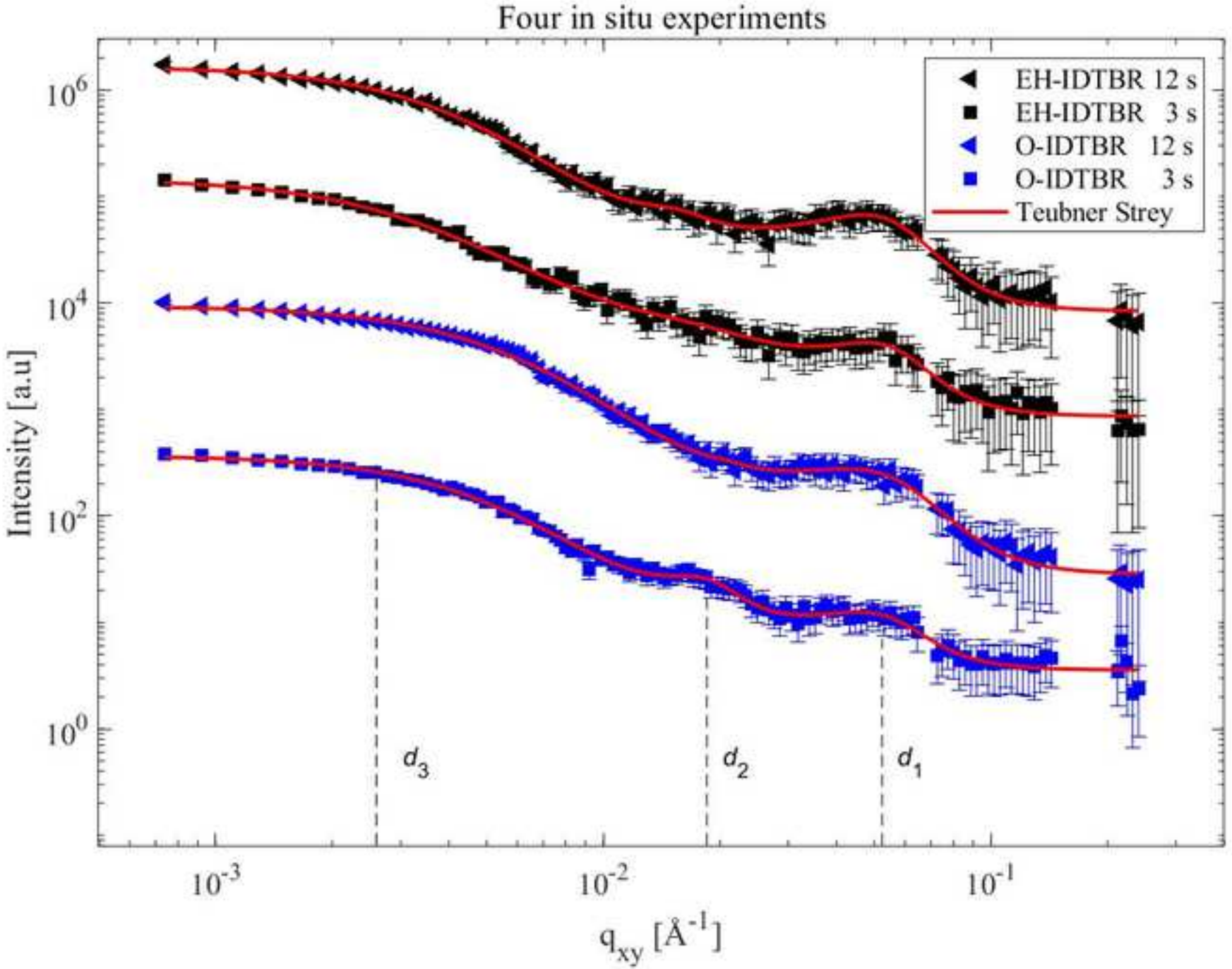

Table 1

	Drying time (s)	Measuring time (s)
P3HT:O-IDTBR	3.0	2732
P3HT:O-IDTBR	12	3000
P3HT:EH-IDTBR	3.0	3000
P3HT:EH-IDTBR	12	3000

Table 2

		PCE (%)	J_{SC} (mA/cm^2)	FF (%)	V_{OC} (mV)
P3HT:EH-IDTBR					
	1	2.20	5.32	59.43	0.70
	2	1.81	4.53	56.97	0.70
	3	1.97	4.83	57.55	0.71
	4	2.17	5.10	60.00	0.71
	5	2.18	5.28	58.49	0.71
	average	**2.07**	**5.01**	**58.49**	**0.70**
	stand dev s	**0.15**	**0.30**	**1.13**	**0.00**
P3HT:O-IDTBR					
	1	3.38	7.95	60.48	0.72
	2	3.33	7.75	60.36	0.71
	3	2.97	7.19	58.72	0.70
	4	3.20	7.48	60.15	0.71
	5	3.24	7.54	60.68	0.71
	average	**3.22**	**7.58**	**60.08**	**0.71**
	stand dev s	**0.14**	**0.26**	**0.70**	**0.00**

Table 3

Fitted values	d_1 [nm]	ξ_1 [nm]	d_2 [nm]	ξ_2 [nm]	d_3 [nm]	ξ_3 [nm]
EH-IDTBR 12s	12.2	4.7	41	22	562	20
EH-IDTBR 3s	12.0	5.0	41	17	225	18
O-IDTBR 12s	12.4	4.8	34	32	489	16
O-IDTBR 3s	12.5	3.9	30	18	241	13

Table 4

Errors	d_1 [nm]	ξ_1 [nm]	d_2 [nm]	ξ_2 [nm]	d_3 [nm]	ξ_3 [nm]
EH-IDTBR 12s	1.4	0.2	10	3.2	11.1	1.7
EH-IDTBR 3s	1.7	0.4	14	2.1	10.3	1.9
O-IDTBR 12s	2.1	0.3	3.5	2.7	9.2	1.5
O-IDTBR 3s	2.2	0.4	12.0	1.3	4.1	0.6

Table of Materials

Click here to access/download;Table of Materials;materialList.xlsx

Name	Company	Catalog Number
Bromoanisole	Sigma Aldrich	104-92-7
Dichlorobenzene	Sigma Aldrich	95-59-1
EH-IDTBR	1-Material	BL3144
Eiger X 4M	DECTRIS	
EQE	PV Measurements	
Flextrode	Infinity PV	Custom order
JV-Measurements	Keithley + JV software	
Mini roll to roll coater	Custom made	
O-IDTBR	1-Material	DW4076P
P3HT	1-Material	M1011
PEDOT	Sigma Aldrich	155090-83-8
PET Substrate	AMCOR FLEXIABLES	
Silver ink	CCI EUROLAM	DuPont 5025
Syringe	Braun	Injekt
Syringe pump	Syringe pump pro	
Tubes	Mikrolab Aarhus A/S	
X-ray source	Rigaku	

Comment
>99.0 %
>99.0 %
10 mm stripes
2000E + JV Software
Slot die coater on a rotating drum
RR 97.6 %
Silver conductor
Rotating anode

Dear Dr. Alisha DSouza,

Thanks for providing us with the opportunity and the two resubmission-extensions to revise our manuscript entitled: *In situ Grazing Incidence Small Angle X-ray Scattering on Roll-To-Roll Coating of Organic Solar Cells with Laboratory X-ray Instrumentation*, to Journal of Visualized Experiments, JoVE. We are thankful for the time and efforts from you and the reviewers to give such thorough and valuable feedback on the manuscript. We believe that addressing the concerns raised by the reviewers have improved the quality of manuscript and thereby its relevance to the readers of JoVE. We have done a major revision of the manuscript to respond to all the comments and concerns from the four reviewers. We would like to thank you for pointing out the framework of a JoVE manuscript. We have done our best to streamline the manuscript in order to fulfil the requirements necessary for publishing in JoVE. During the revision of the manuscript, we found it necessary to include an additional author, Marcial Fernández Castro. He has fabricated the solar cells presented in table 2, which had to be included to address one of the reviewers' comments and he has done a significant contribution during the revision of the manuscript.

Below a line-by-line answer of each comment can be found. Here the original editorial comments and review comments are in black and our responses are in blue. Along with this line-by-line answer, we have attached the revised manuscript and the file with changes from previous manuscript.

We are looking forward to hearing from you regarding our submission and we are happy to respond to any further questions or comments you may have.

Best regards,

Michael Korning Sørensen, Moises Espindola Rodriguez, Marcial Fernández Castro, Ashwin Nambi, Luise Theil Kuhn, and Jens Wenzel Andreasen

Editorial Comments:

• Please take this opportunity to thoroughly proofread the manuscript to ensure that there are no spelling or grammatical errors.

• **Abstracts:** Remove all references from the abstract**.**
The abstract is completely rewritten to not include any references and to address the concern of reviewer #4. We now believe that the abstract is concise and describes the scientific content of the paper.

• **Protocol Language:**
1) Please ensure that ALL text in the protocol section is written in the imperative voice/tense as if you are telling someone how to do the technique (i.e. "Do this", "Measure that" etc.) Any text that cannot be written in the imperative tense may be added as a "Note", however, notes should be used sparingly and actions should be described in the imperative tense wherever possible.
Thanks for pointing this out. We have done our best to write this section in imperative voice.
2) Split up long steps into 2 or more steps.
This has been done.
3) Section 4 needs complete re-writing as a step wise protocol in the imperative.
Thanks for making us aware of this. This section have now been rewritten, such that 6 out of 9 sections are in the imperative tense and in shorter steps. Subsection 4.6, 4.7, 4.8, are still long and not in the imperative tense. This is necessary as these sections addresses the most critical concerns from the reviewers that is essential to know for applying our method. As section 4 is not part of the JoVE narration in the video, and an important part for the readers who will apply this method, we hope that JoVE will accept this format for this short part of the manuscript.

• **Protocol Detail:** Please note that your protocol will be used to generate the script for the video, and must contain everything that you would like shown in the video. Please add more specific details (e.g. button clicks for software actions, numerical values for settings, etc) to your protocol steps. There should be enough detail in each step to supplement the actions seen in the video so that viewers can easily replicate the protocol.
Thanks for pointing this out. We have now written the entire protocol section that goes in the video in imperative tense.

• **Protocol Numbering:** Please adjust the numbering of your protocol section to follow JoVE's instructions for authors, 1. should be followed by 1.1. and then 1.1.1. if necessary and all steps should be lined up at the left margin with no indentations. There must also be a one-line space between each protocol step.
The numbering has been changed to follow the numbering guideline for the protocol and there is now a one-line space between each protocol step.

• **Protocol Highlight:** Please highlight ~2.5 pages or less of text (which includes headings and spaces) in yellow, to identify which steps should be visualized to tell the most cohesive story of your protocol steps. Please see JoVE's instructions for authors for more clarification. Remember that the non-highlighted protocol steps will remain in the manuscript and therefore will still be available to the reader.
1) The highlighting must include all relevant details that are required to perform the step. For example, if step 2.5 is highlighted for filming and the details of how to perform the step are given in steps 2.5.1 and 2.5.2, then the sub-steps where the details are provided must be included in the highlighting.
2) The highlighted steps should form a cohesive narrative, that is, there must be a logical flow from one highlighted step to the next.
3) Please highlight complete sentences (not parts of sentences). Include sub-headings and spaces when calculating the final highlighted length.
4) Notes cannot be filmed and should be excluded from highlighting.
We have highlighted section 1, 2 and 3 in the protocol for telling the most cohesive story of the method/experiment.

• **Discussion:** JoVE articles are focused on the methods and the protocol, thus the discussion should be similarly focused. Please ensure that the discussion covers the following in detail and in paragraph form (3-6 paragraphs): 1) modifications and troubleshooting, 2) limitations of the technique, 3) significance with respect to existing methods, 4) future applications and 5) critical steps within the protocol.
Thanks for pointing this out. We agree that the discussion should be focused on the method in the form of the five sub categories. We have added a few parts to the discussion and rewritten this section to follow the above-mentioned 5 steps explicitly.

• **Figures:** Please remove the embedded figures from the manuscript. Figure legends, however, should remain within the manuscript text, directly below the Representative Results.
These are now removed from the manuscript and fulfil the 300 dpi resolution requirement.

• **Tables**: Please remove the embedded Tables from the manuscript. All tables should be uploaded to the Editorial Manager site in the form of Excel files. A description of the table should be included with the Figure legends.
The tables are now uploaded as Excel files and legends remain in the document.

• **References:**
1) Please do not reference unpublished work (see. Lines 87, 90)
2) Please spell out journal names.
The reference to unpublished work is now removed. In order to justify that we state some of the best efficiencies for large-scale, ITO free, and flexible organic solar cells, we needed to include a co-author on the list. Marcial Fernandez Castro, have optimized the coating conditions for P3HT:O-IDTBR and made the P3HT:EH-IDTBR solar cells that are now added to address the reviewers comments.
We have now used the JoVE reference style.

• If your figures and tables are original and not published previously or you have already obtained figure permissions, please ignore this comment. If you are re-using figures from a previous publication, you must obtain explicit permission to re-use the figure from the previous publisher (this can be in the form of a letter from an editor or a link to the editorial policies that allows you to re-publish the figure). Please upload the text of the re-print permission (may be copied and pasted from an email/website) as a Word document to the Editorial Manager site in the "Supplemental files (as requested by JoVE)" section. Please also cite the figure appropriately in the figure legend, i.e. "This figure has been modified from [citation]."

Comments from Peer-Reviewers:

Reviewer #1:

Manuscript Summary:
This work presents an in situ study of the roll-to-roll coating of organic solar cells by in-house grazing incidence small angle X-ray scattering and intends to be a guideline to perform and analyze in house in situ GISAXS experiments of drying inks on roll-to-roll slot die coated non-fullerene organic photovoltaics. The title, abstract and introduction are adequate and the procedure is well explained with all the materials listed and adequate figures.

We appreciate the kind words and are happy that the reviewer finds the article adequate. We would like to thank the reviewer for raising the following concerns. By addressing these, we consider the quality of the paper much improved.

Minor Concerns:

- **Comment 1:** The manuscript is in general well written although it should be carefully checked in order to correct some mistakes.

  Response 1: Thanks for pointing this out. As part of the revision we have done a careful check to correct all spelling and grammatical mistakes.

- **Comment 2:** Although materials and steps are conveniently listed at some point some more information would be needed. In particular: Why an incident angle of 0.2ºwas chosen? Taking into account the interest of this in house in situ GISAXS protocol and the application for different fields it should be mentioned that optimal incidence angle has to be chosen depending on the sample.

  Response 2: Thanks, these are important observations that we have done our best to clarify. We agree that the incidence angle is an essential part of the experiment and if the readers/viewers would like to adapt this method for a different material system, guidance is needed. For this experiment, the film of interest consist of solvent, P3HT and O-IDTBR. Both P3HT and O-IDTBR have a higher density than the solvent, and presumably has the highest critical angle for total reflection. The critical angle of P3HT and O-IDBTR can vary according to their packing resulting in a critical angle varying from 0.16 - 0.19 degrees, assuming a density of the solid film of 1.1 - 1.35 g/cm3. Thus, 0.2 degrees was chosen to ensure penetration into the bulk of the film. The angle of incidence is important for determining the depth to which the sample is being probed and

whether kinematical or dynamical scattering theory should be applied to model the experimental data. To broaden the relevance to other scientific areas we should also consider how the optimal angle is chosen for an experiment with another materials system. Thus, we added section 3.4 *Choice of incidence angle* (**Lines: 322-328**) to address and clarify this comment and additional references have been included for readers to study the basic theory of GISAXS.

- **Comment 3:** Information on the number of pulses and on the pixel size is missing and it is important regarding resolution and related to the binning process described in the manuscript.

  Response 3: We agree with these observations and find them useful for the readers. The pixel size, sample to detector distance and wavelength have been added to Section 4.4. (**Lines: 301-311**).
  Regarding the number of pulses, we have only used one exposure for the 3000 seconds, integrating the data over the entire exposure time. This has been written more clearly to not mislead the reader: We have clarified this in Section 3.10 (**Line: 266**), where we additionally state that several exposures is a better choice to allow flexible binning of time series.
  The q-scale binning procedure is not unique for this paper and as Reviewer #4 also noted this, we have edited the text and added a reference for this procedure in section 4.5 (**Lines: 313-320**).

Reviewer #2:

Manuscript Summary:
Sørensen et al. report on a step-by-step guideline to prepare, perform and analyze in situ GISAXS experiments of drying inks on roll-to-roll slot die coated non-fullerene organic active layers for photovoltaic applications.

In general, the manuscript is very well written and delivers substantial information to a broader readership. The introduction is essential and synthetic and this facilitates the readability of the paper. The experimental protocol and example results are well described and presented in a complete and clear way. The authors provide adequate experimental information, which might be sufficient to reproduce the experiment or sample preparation from others working in that field, respectively. From the straight scientific point of view, the research in this field is of high interest and progressing quickly.

The manuscript complies with the standards of JoVE and deserves publication after revision of issues noted below.

We are very grateful for such a positive reception. Furthermore, we are happy that the reviewer have addressed some major concerns regarding this demonstration. This will benefit the quality of the manuscript and be of value to its readers. Additional thanks are due for pointing out the needed extension of references cites, as this will surely help the readers to find relevant literature.

Major Concerns:

- **Comment 1:** However, the reference list is not yet adequate. I advise the authors to include and comment on the following publications directly touching their field in the introduction and conclusion section at appropriate positions. Please add few more examples, where the deposition and/or drying kinetics of various coating methods are probed exploiting in situ GISAXS.
  [1] In Situ Grazing Incidence Small-Angle X-ray Scattering Investigation of Polystyrene Nanoparticle Spray Deposition onto Silicon
  By: G. Herzog et al.
  LANGMUIR Volume: 29 Issue: 36 Pages: 11260-11266 Published: SEP 10 2013
  [2] Investigating Polymer-Metal Interfaces by Grazing Incidence Small-Angle X-Ray Scattering from Gradients to Real-Time Studies
  By: M. Schwartzkopf, S.V. Roth
  NANOMATERIALS Volume: 6 Issue: 12 Article Number: UNSP 239 Published: DEC 2016
  [3] Pattern formation of colloidal suspensions by dip-coating: An in situ grazing incidence X-ray scattering study. By: J. Perlich, et al. PHYSICA STATUS SOLIDI-RAPID RESEARCH LETTERS Volume: 6 Issue: 6 Pages: 253-255 Published: JUN 2012
  A recent publication is also reporting on morphological and performance effects of Solvent Additives during slot die printing of nonfullerene acceptor based organic solar cells.
  [4] Effect of Solvent Additives on the Morphology and Device Performance of Printed Nonfullerene Acceptor Based Organic Solar Cells. By: K.S. Wienhold et al. ACS APPLIED MATERIALS & INTERFACES Volume: 11 Issue: 45 Pages: 42313-42321 Published: NOV 13 2019

  Response 1: Thanks for pointing this out, we agree with the reviewer on this. We have included the 4 articles that are listed above because of their relevance in the field and context with respect to the described method. Additionally, 23 articles have been cited to complete the argumentation for the work presented here and to proper respond to the concerns addressed by the four reviewers. We believe that the reference list is now adequate for publication. Furthermore, we believe this will help the readers finding more literature that can guide them to adapt this to their own materials system or coating technique.

- **Comment 2:** Please comment on potential X-ray beam effects and large scale morphological homogeneity of the printed active layers.

  Response 2: It is expected that the large-scale morphology is changing over time as the analysis also confirms. In this article, we have probed a drying film after 3 and 12 seconds of drying, the only way to do this is to probe fresh film all the time. The morphology is expected to vary over the length of the foil, and as we are coating 18 meters of active layer, the first meter may very well be different from the last one. For our experiment we do not have the flux (time resolution) to probe this and we have to accept that the observed structure represents a mean of the 18 meters of coated foil. For future experiments, we recommend shorter exposure times to allow flexible binning of time series that will allow large-scale inhomogeneities to be identified (This have been added to Section 3.10 (**Line: 266**). If one wishes to probe variations on smaller time or spatial scales, a synchrotron source is needed to have the required flux that is not available from a laboratory X-ray source. This point we have added in the discussion section 2 (**Line: 425-428**)

  Regarding X-ray beam damage, we believe that it can be neglected due to the low flux and the low residence time of sample in the beam.

- **Comment 3:** How does the roll-to-roll process induce temporary misalignments of the incident angles and thus change of beam size and penetration depth during the roll-to-roll process and does it affect the GISAXS measurements respectively analysis.

  Response 3: This is a very good point which has also been raised by reviewer #1 and #4. The incidence angle is particularly important when performing a grazing incidence small angle X-ray scattering experiment (GISAXS). Previous synchrotron experiments where this roll-2-roll coater has been used have demonstrated that the incidence angle does not vary more than ± 0.03° as evaluated by the position of the reflected beam as a function of time (with a temporal resolution of 0.1 s), which is equal to ± 12 pixels from the Yoneda line for this experiment, whereas, the horizontal line integration were made with ± 50 pixels. Under the assumptions made for this analysis and the fact that the horizontal line cuts are integrating angles that are larger than this uncertainty it is fair to assume that it will not influence the analysis. In future work (as reviewer 4 suggest), the beam-stop should be excluded to allow tracking of the reflected beam, thus improving the possibility of making post-acquisition corrections. To address this with the current experiment, subsection 4.4 and a paragraph in the discussion part 1 has been added. **Lines 399-410 and Lines 201-311.**

- **Comment 3:** Please comment on potential additional challenges while printing on hot foils like turbulent hot air convection or higher solvent evaporation rates.

  Response 3: This is an important point, especially when comparing this data with other experiments. We agree that temperature and airflow will influence the drying of the film. Each data point presented here were acquired under same coating conditions (temperature of foil and ink, foil speed, exhaust rate), thus they are subjected to the same environment and an internal comparison is valid. It is expected that changing the environment will influence the drying and in future experiments we recommend that environmental parameters are recorded (relative humidity and airflow above the substrate.). We have addressed this concern in the discussion. **Line 412-417.** Additionally, we have stated the importance of this during the installation of point suction in section 3.6, to notify the reader that point suction should be stable throughout an experiment. **Line 247-249**

Minor Concerns

- **Comment 4:** Please specify beam size and foil size in beam direction at 0.2° incident angle at the sample position.

  Response 4: The beam size is now stated in section 3.1. **Line 203 - 215**.

- **Comment 5:** In addition environmental parameters like temperature and relative humidity are worth mentioning for reproducibility.

  Response 5: The experiments were carried out in a temperature controlled laboratory at a constant temperature of 22° C, whereas the relative humidity was unfortunately not noted down at the time of the experiment. The implications of the relative humidity is particular important for reproducing these experiments elsewhere as now emphasized in the discussion section in **Lines 413-419**. As for the internal comparison in this paper, it is fair to assume that humidity was the same for all four measurements.

Reviewer #3:

The article by Sorensen et al. describes the procedure of carrying out in-situ GISAXS to characterize the morphology kinetics in roll-to-roll coating of OPVs. It was well written with sufficient background and experimental details. I think it is suitable for publication in JoVE provided several minor revisions.

We thank the reviewer for the positive reception of our manuscript. We appreciate that the reviewer have read the manuscript carefully and therefore have some valuable comments that has led to improvement of the manuscript.

- **Comment 1:** Lack of description of flatness (wobbling during rolling and substrate wrinkling) control and its effect on quantitative characterization. The uncertainty in the incident angle matters if it varies too much. Maybe this can be done with some dry runs without ink deposition?

  Response 1: Thank you for raising this important issue. The incidence angle is very important for a GISAXS experiment and the reviewer has a good point that this must be documented. As suggested by reviewer #4 this can be done by removing the beam stop and tracking the specular beam position throughout the experiment. In the experiments we report on here, we do not have a time resolved tracking of the specular peak. This will be done for future experiments. In previous synchrotron experiments where this roll-2-roll coater has been used we have demonstrated that the incidence angle does not vary more than ± 0.03° as evaluated by the position of the reflected beam as a function of time (with a temporal resolution of 0.1 s), which is equal to ± 12 pixels from the Yoneda line for this experiment. The horizontal line integration were made with ± 50 pixels. Thus we find the small variation neglecteable for the purpose of this analysis. This have been addressed in the discussion **Lines 399-409.**

- **Comment 2:** I do not see the need of figure 5b if no GIWAXS is discussed elsewhere.

  Response 2: Thanks for reading this so carefully. This is a misspelling: It is GISAXS. It has now been corrected.

- **Comment 3:** Are those long exposures (3000 sec) done with a single shot or repeatedly multiple shots?

  Response 3: This is done by one long exposure of 3000 seconds. Improvements of this experiments will be to collect data with several shorter exposures to ensure data quality and to allow flexible temporal binning. We have added section 3.10 to clarify this. **Line 266 + note**

- **Comment 4:** On ~425nm films prepared by slot-die, I expect the morphologies are more of 3D rather than 2D only in the surface plane. Therefore, the structure analysis should be done as a function of total q (not qy, especially when the linecut is done at a non-zero qz). If it is believed to be 2D, then linecuts of qy at different qz are needed for validation.

  Response 4: Very good observations that we acknowledge the importance of. The structure is expected to be 3D. But for this analysis we have restricted the analysis to

the horizontal features and we cannot retrieve a full 3D information about the structure in the bulk. We have made integrations 30 degrees rotation from the $\mathbf{q}_{xy}$ plane and which showed features at the same q-length as for the horizontal integrations, but here the Teubner-Strey model is not valid due to refraction and reflection terms. Therefore this analysis is solely focused on the horizontal domain sizes. To retrieve a full 3D size distribution map requires more sophisticated models as we have described in the discussion: **Line 463 – 477**.
The horizontal line cuts have been made at the Yoneda line as described and are only done in $\mathbf{q}_{xy}$ because here we can neglect the reflection and refractions terms. This we have further clarified in the text and added a few references that provides support of the applicability of this method: **Line 300 - 309**.
We further added a subsection 4.6 and subsection 4.7 to clarify and justify this as it is crucial for our argumentation for using the Teubner-Strey model. **Lines 322 – 339**.

- **Comment 5:** Please plot the GISAXS image in logscale or enhance the contrast in Figure 9, and label the axes with qy/qz or exit/in-plane angles, so one can see the overall peak feature locations that lead to the bumps in the 1D linecut. This will directly give information on overall morphologies, especially whether the morphology is 2D or 3D.

  Response 5: Good suggestion, this will increase the readability. This figure have been updated accordingly (figure 9).

Reviewer #4:

Manuscript Summary:
Sorensen et al show in their manuscript how to use a lab source to still access time-resolved, structural information for GISAXS measurements on OPV thin films that are carried out over long exposure times. They sketch their approach and demonstrate the feasibility of the measurements using two binary systems.

The experimental design is indeed highly valuable if access to synchrotrons is not possible. However, a large amount of material is necessary as the authors point out.

We are very grateful for the positive acknowledgement of our work. We are happy that the reviewer did such a thorough read to raise all these concerns, regarding both the scientific and the communicative aspects of this manuscript. Furthermore, the reviewer have made some good comments that we will apply to adapt our future work – thanks.

General Concerns:

- **Comment 1:** While the topic of the manuscript is very exciting the presentation promises more (need to solve control of morphology, resolve drying kinetics - with two data points?), than is presented in the end. This is a pity. A more down to earth approach in the formulation, with some added scientific details would make the manuscript a much more enriching experience to read.

  Response 1: Thank you for addressing this. We completely agree and believe that this is a fair point and it will be a pity if we disappoint the readers, which is clearly not our intention. We intend to give a general introduction to the research field and to motivate why performing in situ GISAXS is relevant to pursue the fundamental structure-property relations for organic solar cells. We have rewritten the abstract completely and emphasized the development of the roll-to-roll GISAXS technique. We now think it is clearer in the sense that this paper demonstrate a method that do not provide the answers for the optimal morphology for organic solar cells, but a tool to investigate the structure-property relations.

- **Comment 2**: The introduction could be cut a lot more (anyone attempting to realize such a measurement would already have that very basic background at this stage?) and allow for much more room to detail the set-up itself. Which would still be necessary if one wanted to reproduce these results. Overall, I would recommend some major revisions to make this manuscript more precise and more valuable to the readers.

  Comment 2: Thanks for the comment. We have attempted to revise the manuscript considerably to ensure that people can replicate the results. Regarding cutting the introduction, we do not assume that the readers have the basic background before reading/viewing this article/video. We believe that the introduction is both necessary and indeed helpful for the readers of JoVE, where we expect that most readers start by viewing the videos and then subsequently reads the article, if they find it relevant. For people who use GISAXS on a daily basis this might not contribute with much to their knowledge, but for people new (less than 3 years of PhD study) in the field of either OPVs or GISAXS, we believe that the information provided in the introduction is of value. Additionally, if the reader want to apply this roll-2-roll GISAXS technique to another field than OPV, we believe that this serves as good inspiration for making this applicable for other research fields.
  Regarding the reproducibility, the protocol has now been further detailed to ensure that the readers can perform such an experiment themselves.

Comment 3: Further, here are some more detailed questions, that arose when I read the manuscript: The authors show that the EH-IDTBR system results in various pinholes. Pinholes in the active layer of an OPV device are known to reduce the efficiency. Can the

authors please include information on the size and geometry of the solar cell device. Particularly whether there are more inactive pixels for one material type than the other. This is necessary to actually conclude anything on the material itself and not just to the differing degree of defects.

Response 3: We are grateful for this observation. We believe it improves the quality of the article to address these questions. We have included information on the geometry and the size of the solar cells as well as the various layers involved. As we used an easily scalable roll coating platform, the pixels for each material type are individual solar cells of 1 cm^2 of photoactive area. **Line 79 – 88.**
The pinholes in the P3HT:EH-IDTBR material system are covered by the subsequent PEDOT:PSS layer during the solar cell fabrication avoiding any possible short circuiting of the devices, however resulting in devices with a larger variation of the solar cell performance. In table 2, we have added the average and standard deviations of the key solar cell parameters.

- **Comment 4:** What is the actual amount of material necessary for such an experiment? A rough number to carry out optimization and the experiments would be helpful for decisions of feasibility. Information on the solar cell fabrication is not sufficient for reproducibility.

  Comment 4: The actual amount of material is stated in section 1 of the protocol **Line 152**. We have added the structure of the final device. A full description of fabricating these solar cells is worth an article of its own. Such an article is currently under revision with another journal where all the details are described. We hope that we can cite it in the proof of this paper such that people can find the paper when reading this. For now, we have made references to a similar coating technique done by the group of Prof. Frederik Krebs **Line 79 – 88.**

- **Comment 5:** Section 3.3. It is well known that shifting the beam on the aligned sample (here height change at the end to optimize the signal) will result in a change of incident angle on non-flat surfaces. I would expect the flexible substrate to be not perfectly flat. Could the authors please comment on how accurately they can align the sample on these flexible (and moving) substrates.

  Response 5: Very good point! Reviewer 1 and 2 addresses this as well. From previous synchrotron experiments where this roll-2-roll coater has been used we have demonstrated that the incidence angle does not vary more than ± 0.03° as evaluated by the position of the reflected beam as a function of time (with a temporal resolution of

0.1 s), which is equivalent to ± 12 pixels from the Yoneda line for this experiment, whereas the horizontal line integration were made with ± 50 pixels. Thus, we find the small variation neglectable for the purpose of this analysis. This have been addressed in the discussion **Lines 398-410.**

- **Comment 6:** Section 3.4. Could the authors please specify why the use of a beamstop increases the signal to noise measurement for an EIGER detector? This used to be the case for older detector technologies, but shouldn't actually be the case for the dectris detector used here. It should also easily withstand the quoted flux, such that I do not yet see the advantage of the beamstop. The direct beam could be used for tracking the stability of the set-up (e.g. fluctuations of the substrate).

  Response 6: Very good suggestion! We are thankful for the comment since this will be the practice from now on, thanks.
  First, it is true that it will not increase the signal to noise ratio. We have now removed this part from the manuscript, as it is indeed an incorrect statement.
  In retrospect, a beam stop (blocking both the direct and the reflected beam) should not have been used for this experiment. We could then have used the specular peak to track the incidence angle to prove the stability of our measurements. We have added a new subsection 3.5 to highlight this. **Lines 240– 246.**

- **Comment 7:** Section 3.5. Is the sample environment open to the optics and toward the detector? If not, what type of windows are used to ensure the solvent atmosphere doesn't harm the equipment? How is "ensured" that the suction does not influence the drying? (Solvent atmosphere can significantly alter the drying process (Proeller et al, 10.1063/1.4984130).

  Response 7: The sample stage is in ambient conditions and the entire X-ray set up is in vacuum. We use 10 µm thick mica windows. The solvent atmosphere is expected to be the same for all 4 experiments performed as the exhaust, solvent and temperature are the same. Thus, it can be assumed that the flow is constant for all four experiments and therefore an internal comparison of the four experiments shown here is valid. It is true that moving to another instrument or changing the solvent or exhaust will require a thorough documentation to allow for comparison. This is a good argument and we have added a few paragraphs and the suggested a reference to address this in the discussion. **Line 411 - 414.**

- **Comment 8:** Section 3.8. What type of camera is used to monitor the sample to obtain detailed enough information without strong reflections and to actually observe the drying front to judge the quality of the printing run?

Response 8: The camera used here is an AUSDOM AW620 1080p webcam. This is used to observe the total width of the coated film and to visually track de-wetting. This have been specified in section 3.11. **Line 266**.

- **Comment 9:** Section 3.9. Since the aim is to understand the drying kinetics of inks, it should be made clear on how the time resolution is being achieved.

  Response 9: Very good point. If this is not clear in the text it is our fault as it is essential to understand the experiment. This should be stated more clearly in the text. The two drying times stated in the article, 3 and 12 seconds, were thus achieved: The tip of the coating head is placed 12 cm from the X-ray beam, the moving substrate has as speed of 1 cm/s, thus the probed film have been drying for 12 seconds. We have added the details in section 3.8 **Line 254-258.**

- **Comment 10:** Section 4.2. How has the data correction process been adapted for the GISAXS geometry from the SAXS reference? E.g. background subtractions are not necessarily valid for GISAXS.

  Response 10: This is a good point. We agree that this was not clear in our formulation and it would have mislead the reader if not corrected. We have only applied the corrections that are applicable for GISAXS as well. We have rewritten this section accordingly. **Line 286-290**.

- **Comment 11**: Section 4.3. It should be mentioned that the horizontal line cut is done at the yoneda region. (e.g. Hexemer 10.1107/S2052252514024178) Furthermore, for the method presented here it should be evaluated, how precisely the Yoneda region can be determined due to the moving substrate.

  Response 11: This is very good point and we have specifically addressed this by referencing the stated article with others and added two paragraphs in section 4.4, **Line 300 – 311.** Additionally, we have changed equation (3) to explicit show that the model is applied in the q_{xy} direction.
  The second part of the question is concerning the moving substrate. From previous synchrotron experiments where this roll-2-roll coater has been used we have demonstrated that the incidence angle does not vary more than ± 0.03° as evaluated by the position of the reflected beam as a function of time (with a temporal resolution of 0.1 s), which is equal to ± 12 pixels from the Yoneda line for this experiment, whereas, the horizontal line integration where made with ± 50 pixels. Thus we find the small variation neglecteable for the purpose of this analysis. This have been addressed in the discussion **Lines 398-409**

- **Comment 12:** 4.4. Logarithmic binning is standardly done (e.g. Proeller 10.1002/aenm.201501580)

  Response 12: Good point, we have rewritten section 4.5 **Line 312-319** to describe this with reference to the suggested article.

- **Comment 13:** Section 4.5. On which basis do the authors claim that the used fitting model by Teubner and Strey is valid for GISXAS measurements? Here, reflection and refraction terms also need to be taken into account (e.g. Babonneau 10.1107/S0021889810020352).

  Response 13: This comment is particular relevant and we found it necessary to add another two subsections in the analysis section to address and clarify the assumptions and references needed to perform the analysis presented here.
  Subsection 4.6) Assumptions necessary for applying the Teubner-Strey model for GISAXS analysis **Line 321-327**, and subsection 4.7) Argumentation for applying the Teubner-Strey model **Line 329 – 338.**